Control of a multi-robot cooperative team guided by a human-operator

eingereichte
MASTERARBEIT
von

cand. ing. Martin Angerer

geb. am 10.06.1991
wohnhaft in:
Steinheilstrasse 5
80333 München
Tel.: 0151 57978548

Lehrstuhl für
INFORMATIONSTECHNISCHE REGELUNG
Technische Universität München

Univ.-Prof. Dr.-Ing. Sandra Hirche

Betreuer: Selma Musić, M.Sc.
Beginn: 01.10.2015
Zwischenbericht: 21.01.2016
Abgabe: 15.06.2016

In your final hardback copy, replace this page with the signed exercise sheet.

Abstract

Interaction between humans and robots in cooperative manipulation expands the range and complexity of admissible tasks. A shared control approach allows the user to teleoperate the overall formation, while the robots establish their coordination autonomously. Human-in-the-loop stability proofs in telemanipulation usually base on a dynamic model of the human arm manipulating a reactive input device.
In general the human behaviour is unknown and user interfaces, like gesture recognition control or motion tracking, allow for arbitrary inputs, which are possibly unsafe or unstable. Without a model of the human behaviour, control design must ensure stability regardless the user's commands. In this thesis we design a model-based controller, that uses virtual structures to coordinate robot motion and to virtually couple the human operator. The port-Hamiltonian formulation of the controller unveils its energetic state, which is used to adapt the (virtual) coupling of the operator. An energy tank passivates the coupling and limits the energy stored in the controlled system.
The control scheme is proven to be intrinsically passive and achieves stability with any user input. Collision safety for humans on-site is enhanced by the limited stored energy. Simulation results validate 1) the coordination preservation of the robots, 2) the overall trajectory following, 3) the energy-bounding of the controlled system.

Zusammenfassung

Die Interaktion des Menschen mit einem Team kooperativ arbeitender Roboter erweitert die Vielfalt und Komplexität möglicher Aufgaben. In dieser Arbeit wird der Ansatz einer Regelung mit geteilten Zuständigkeiten gewählt. Das ermöglicht es dem Benutzer die geschlossene Formation der Roboter direkt zu lenken, während diese ihre Koordination eigenständig herstellen. Die weitgehend unbekannten dynamischen Eigenschaften des Menschen, zusammen mit einer nicht-restringierenden Eingabeschnittstelle, erfordern die Berücksichtigung beliebiger Befehle, einschließlich unsicherer und/oder instabiler.
Es wird ein modell-basierter Regler vorgeschlagen, aufgebaut aus einer virtuellen Struktur, die einem kooperativ-greifendem Ansatz gleicht. Diese sorgt für die Koordiation der Roboter und bindet gleichzeitig den Benutzer ein. Das Regelschema ist intrinsisch passiv und simuliert den energetischen Zustand des geregelten Systems. Daher erfolgt die Systembeschreibung mit dem port-Hamiltonschen Ansatz.
Die Information über den Energiezustand wird zur dynamischen Anpassung der Kopplung des Benutzers verwendet. Damit wird ein sicherer und stabiler Zustand des Systems erreicht. Stabilität, aber keine asymptotische Stabilität, wird dadurch sichergestellt. Die Anwendung energiebasierter Sicherheitskriterien führt zu einem ungefährlichen Verhalten im Falle einer Kollision mit einem Menschen.

Contents

Chapter 1

Introduction

Interaction between humans and robots expands the range and complexity of admissible tasks in a natural way: humans come with superior foresight and planning capabilities, while being inherently robust and adaptive in unexpected situations. On the other hand, robots perform tasks repetitively and with high precision. In addition, robots can operate in areas humans cannot (space, hazardous environments). Remote human control, i.e. teleoperation, of the robots combines human cognition with robotic strength. Multiple robots working together in a cooperative team are capable of carrying out more complex tasks with less specialized tools. The prime example is grasping and transportation of large and/or heavy objects. Other options are the coordinated use of tools and the assembly of multiple parts without using special fixtures [CM08].
For several teleoperated robots in a cooperative team a variety of feasible control topologies exists. Dependant on the role of the human in the control loop and the level of autonomy of the robotic team, we distinguish three classes of architectures: direct, shared and supervisory control [HB12]. In direct control approaches humans operate each robot separately by manipulating a haptic device, e.g. [Goe52]. On the other hand, applying supervisory control, the robotic teams act autonomously and the operator issues high-level commands, e.g. "relocate to a certain place" or "grasp an object" [PST+15]. The operator continuously receives information on the state of the robotic system and periodically issues commands, thus rather oversees and directs than controls the system [She92]. The intermediate between supervised and directly controlled systems are shared control systems. At least some local, low-level feedback loops refine the robot behaviour to assist the operator in high-level task execution [NPH08]. One natural evolution of shared control for multiple robots is the leader-follower paradigm. The leader (in our case the human user) is not physically coupled to the robotic team, but virtually directs the robotic followers. The formation of the robotic followers is established automatically (low-level task), thus the user can focus on guiding the closed formation (high-level task). In contrast to supervisory control the human is directly included in the control loop and her/his dynamic behaviour affects the overall stability.

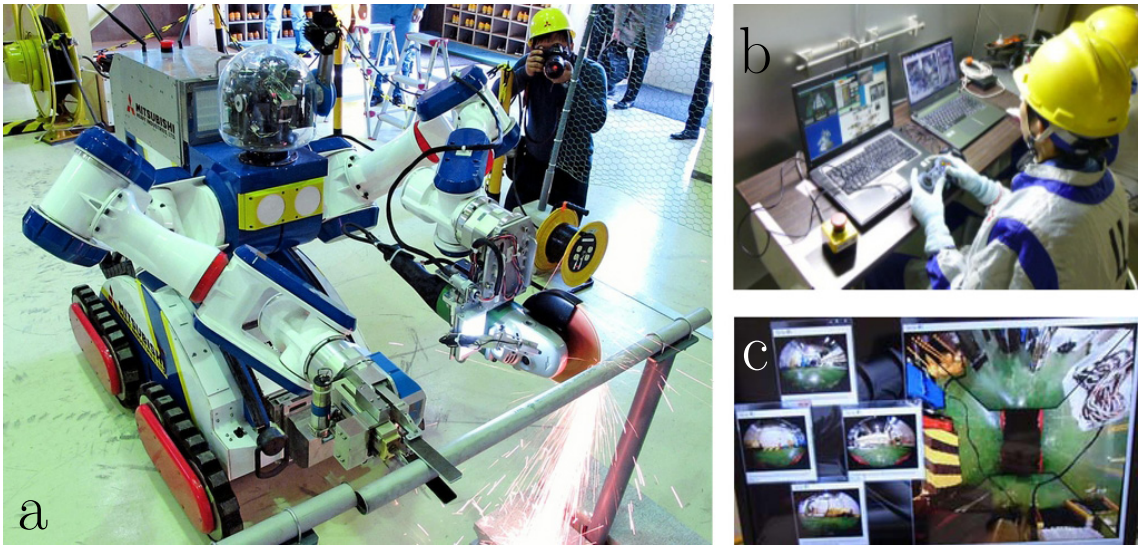

Figure 1.1: Demonstration of the teleoperated MHI MEISTeR robot at Fukushima Daiichi Nuclear Power Station [Ind14]: a) the robot carrying out a coordinated use of tools task b) operators using video game controllers c) visual feedback for the operator as displayed on the computer screen

The virtual integration of the human into the robotic set-up requires an interface that formalizes the indirect human-robot interaction. A common user interface in robotic teleoperation is the master-slave relation. The master-device is manipulated by the human and the slave-robot follows its motions. This is frequently used for the direct control of a single robot but also in shared control of a cooperative team [LS05]. It is also common for master-slave systems to provide reactive force-feedback to the user, i.e. the force necessary to conduct the commanded motion is reflected to the operator and impacts the human motion. In such a set-up the human hand is modelled as a mechanic impedance [Hog89]. In supervisory architectures the user typically directs the system via a data processing station on a higher level [PST+15]. For shared control many conceivable interfaces exist, e.g. motion capturing [SMH15], hand gesture recognition [GFS+14] or video game controllers (see figure 1.1). The latter are used to control a teleoperated robot inside the Fukushima Daiichi Nuclear Power Station. The robot shown in fig. 1.1a is equipped with two arms to cooperatively manipulate tools.

The aforementioned input methods have in common that the user is not provided with reactive force-feedback. There is no counteracting force or maximum deflection barrier to limit the possible inputs, thus the user may command arbitrary trajectories. Consider a robotic set-up driven into an obstacle and a user persisting to command motion in the blocked direction. Contact forces and desired velocity become an infinite source of energy. Thus it is indispensable to consider commands that may destabilize the system and/or endanger the environment, especially humans on-site.

Concerning safety, a number of collision detection and response strategies exist to make the robot behaviour safe when it comes in contact with a human [Had14]. These methods work well for slow motion, but for fast and sudden impacts the closed-loop bandwidth of the robots is too slow. The robot's dynamics is then dominated by its effective inertia [LTC12]. A general solution is to limit the energy stored in the robotic set-up. In an unexpected collision the exchangeable energy is then bounded [TdVS14]. Empirical studies relate severe injuries of humans to the energetic state of the robot [Woo71, YPM+96].
Towards a conclusion on closed-loop stability of such a set-up, the major challenge is the unknown dynamic behaviour of the human and the non-restrictive input interfaces. Seen from a control point of view, the human decision making is a "black box", the inputs and outputs are available, but the internal behaviour is unknown. Psychological models based on empirical studies and neural network structures [PST+15] emulate human behaviour. However, there is no way to guarantee successful modelling of the unpredictable human behaviour. Thus they do not qualify to be the base of a stability proof of the closed-loop behaviour.
The objective of this thesis is two-fold: first, a shared control architecture for cooperative object manipulation is designed. We apply the leader-follower paradigm, where a human commands the object motion, while the robots autonomously maintain the coordination (chapter 2). The controller is passive, i.e. is asymptotically stable with any environment iff the energy supply is finite. Therefore the second goal is an energy shaping approach to cope with an unmodeled human in the loop, who can command arbitrary trajectories and thus supply infinite energy. Bounding the energy in the system ensures closed loop stability and enhances the safety for humans in the environment of the robots (chapter 3).
Energy is a major entity in this thesis, a power-consistent formulation allows insights into energy flow and facilitates stability proofs. Thus it is functional to choose an energy-based system description. The port-Hamiltonian representation additionally allows a model-based controller design.
Chapter 2 starts with a general introduction to the port-Hamiltonian framework and details on the description of 3D-mechanical systems. By interconnection of virtual mechanical elements we design two model-based controllers.
Chapter 3 introduces an energy tank to limit the energy supply to the controllers designed in chapter 2. We propose an adaptive coupling of user and robots to shape the energy exchange dependent on the tank level.
Chapter 4 presents simulation results of the schemes developed in chapter 2 and compares them to known approaches. The effectiveness of the energy-bounded trajectory tracking is also verified by simulation.
Chapter 5 draws a brief conclusion and some remarks on future directions are given.

1.1 Problem Statement

Multiple robots manipulate a common object, the human user guides the formation by hand motion. There are two major challenges to be considered in this type of human-robot team interaction: 1) How to address the coordination of the multiple robots in order to let the operator focus on object motion; 2) How to achieve stability and safety with the human in the loop.
The full set-up of human-robot team interaction we want to analyse and model is shown in figure 1.2. The user does not interact physically with the robots, but is virtually coupled in the manner of a leader-follower scheme. When cooperatively handling an object, the robots need to preserve a certain formation to avoid dropping or excessive squeezing of the object. Thus the controller has two tasks, 1) to ensure trajectory following with respect to the human motion (high-level task), 2) to generate suitable trajectories for each robot to respect the coordination requirements (low-level task). The control scheme to be designed is thus shared, since it has an autonomous part (formation preservation) and a human command part (movement of the formation).
In such a shared control set-up the control loop encompasses the human and the environment the robot team interacts with. Towards stability and safety the major challenge is the largely unknown dynamics of both human and environment. Input interfaces that do not restrict the human commands, either by a counteracting force, or maximum deflection, allow for infeasible and/or unsafe trajectories. It is the objective of the controller to achieve safe and stable operation for arbitrary inputs.

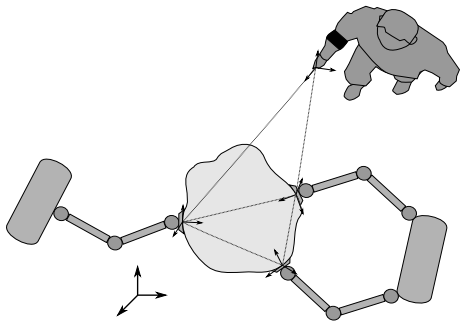

Figure 1.2: A human user interacting with a robotic team cooperatively grasping and manipulating an object

1.2 Cooperative manipulation and energy regulation control

A number of classic control schemes for cooperative object manipulation are object-centred and therefore qualify for shared control approaches. They use the so-called *grasp matrix* to relate object and manipulator motion and force distribution [CM08]. The first to use also the impedance control paradigm [Hog84b] in cooperative manipulation tasks are Schneider and Cannon [SC92]. They establish a compliant relation between the desired and the actual object pose. Bonitz and Hsia [BH96] use an impedance relation between the object and each manipulator. This is essential to ensure stability during contact and non-contact transitions. Both impedance relations are combined in [CV01, CCMV08] and more recent in [HKDN13]. Notably the latter elaborates on (asymptotic) stability of the control scheme with a known environment.
The mentioned control schemes employ second-order impedance control to achieve a very dynamic trajectory tracking but are not passive. The cancellation of open-loop dynamics generates possibly unbounded energy. Stramigioli [Str15] points out the effectiveness of passivity when dealing with unknown environments, as for every non-passive controller a passive environment exists that destabilizes the overall system.
Stability with unknown environments, which can only supply a limited amount of energy, is achieved by the *Intrinsically Passive Controller* [Str01b]. The original version has no dampers in parallel with the springs and thus has a weak dynamic performance. Different implementations on the DLR Hand II [WOH06, WOH08] add the dampers along the springs. Instead of using the grasp matrix to describe the kinematic relations of object and manipulators, a virtual structure with a simulated object is introduced. Virtual structures are a well known tool in *formation control* to establish a certain geometric shape of several robotic manipulators [LBY03]. Virtual springs and dampers are used in [VSvdSP14] to coordinate the formation driving of a group a wheeled robots. The Intrinsically Passive Controller features a virtual structure of springs, dampers and a mass (the virtual pendant of the common object). Asymptotic stability follows from the passive nature of the (virtual) mechanical elements [Str15]. Recently, Sieber et al. [SMH15] establish formation control of several manipulators around a common object and study the control options for a human to direct the closed formation.
A human operator is easily included in the formation by virtual spring coupling, especially when in a leader-follower scheme [SMP14]. The human leader can be virtually connected to all or some robots [SMH15], a certain point (e.g. the geometric center of the formation) [WOH06], or an element of the virtual structure (e.g. the manipulated object) [Str01b].
The concept of passivity is widely used when including a human in the control loop [HB12]. Passive systems either store or dissipate supplied energy, i.e. they reach an energetic equilibrium, iff the energy supply is finite. Thus the only requirement

to achieve stability with a passive robot team is, for the human, to supply only a bounded amount of energy [Str15]. To guarantee that only a certain amount of energy is available, an *energy tank* replaces the human to provide energy to the robots. When combined with a proper re-filling strategy the tank concept effectively limits the rate of energy exchange. Known applications of tanks are variable rate haptics [LH10] and teleoperation over delayed communication lines [FSM+11]. Re-filling is necessary because performing actions on the environment usually consumes energy, i.e. energy is permanently withdrawn from the system.
In addition, a tank sourced system can be controlled dependent on its energetic state. The general concept, of actively stabilizing a system at a certain energy level, is usually called *energy shaping control* [OvdSME99]. The energy stored in a robotic system is also a benchmark for possible injuries when it comes to a collision with a human [Woo71, YPM+96]. Approaches to maintain a safe level in single robots modify the given reference trajectory [LTC09], or adapt the internal behaviour of the robot [TdVS14]. Very recent, energy shaping for safety reasons is proposed for a robotic team, that is physically coupled to the human [GSDLP16].
The methodology of energy regulation for teleoperated robotic teams is largely unexplored in literature. Neither are there safety evaluations for cooperative object manipulation tasks. Safety concerns are appropriate because of the higher moving inertias (and thus kinetic energy) in such a set-up. If a user interface allows arbitrary trajectories to be commanded, some require infinite energy for the execution, then passively controlled robots are not sufficient to conclude stability. To the best of the author's knowledge this problem has not been considered so far.

Chapter 2

port-Hamiltonian modelling

In this chapter we introduce a modelling approach of the cooperative system in the port-Hamiltonian framework. This formulation is based on energy, a major entity in this thesis. Throughout this chapter it will be clear how energy consistent modelling facilitates control design, allows insights into the flow of energy in the system and provides a ready-made stability proof. The first section is dedicated to illustrate these advantages in more detail. The general theory of port-Hamiltonian systems is presented in section 2.2 and its generalization for six-dimensional mechanical systems in section 2.3. An elementary module in mechanical systems are spring-mass-damper systems, as they reproduce a compliant contact. Their construction in section 2.4 is an example how the systematic interconnection of the atomic mechanical elements works. The counterpart of a compliant contact, namely the rigid contact is treated in section 2.5. Then we have all the preliminaries to model a cooperative manipulation set-up. Inspired by the virtual structures to achieve a group behaviour in formation control [LBY03], we design a model-based controller in the last section 2.6.

2.1 Energy-based modelling and control

Every physical process involves energy and especially energy transfers or transformations. Energy is a very general concept in physical systems, it allows for a consistent description across different physical domains. Even within the mechanical domain there are two forms of energy (kinetic, potential), e.g. acceleration can be viewed as a transition from potential to kinetic energy. Energetic relations do not only define static relations between physical systems but also their dynamic behaviour, described by the transient exchange of energy [OvdSMM01]. The modelling of a complex physical system can therefore be accomplished by an interconnection of simple subsystems, defined by an energy function. We can combine such physical elements to achieve a desired dynamic behaviour and thereby define a model-based controller on energetic level. In contrast to this, control is traditionally handled from a signal processing viewpoint. Starting from a reference input, an output signal is generated to reduce some error signal. Control design on the energetic level

allows to build a model-based controller in a physically meaningful way. An energetically consistent control scheme visualizes the flow of energy in the system (e.g. energy supplied by an operator distributed to the robots) and is intrinsically passive. Considering the energy balance of the controlled system and explicitly performing control by shaping the energy is the foundation of passivity based control. Passive controlled robots are appropriate when dealing with unknown environments (see also chapter 3 and [Str15]).
Another motivation for control design on energy level is safety in physical human-robot interaction or co-working. The kinetic energy stored in the robotic system is intimately connected with the risk of severe injuries of a human. Assume a human explicitly controlling a robotic team, by her/his commands s/he supplies energy to the controller and the controller distributes the energy to the robots. Because of its formulation on the energy level, the controller is aware of the energetic state of the system and can adapt its behaviour to keep the energy bounded (see chapter 3).
For the energy-consistent modelling of mechanical systems two approaches are known: the Lagrangian and the Hamiltonian. In recent years a combination of the Hamiltonian description and port-based interconnection was developed, we refer to port-Hamiltonian modelling. It allows to describe complex physical systems based on the interconnection of simpler subsystems, represented in a convenient input-state-output formulation, which has the structure of a (non-linear) state space formulation. The Hamiltonian function of the interconnected system sums up the total energy stored in the subsystem and is a Lyapunov candidate function, facilitating stability proofs.

2.2 port-Hamiltonian description of mechanical systems

For the derivation of the port-Hamiltonian description of a mechanical system we start from the classical *Euler-Lagrange* equations of motion

$$\frac{d}{dt}\left(\frac{\partial \mathcal{L}}{\partial \dot{\boldsymbol{q}}}\right) - \frac{\partial \mathcal{L}}{\partial \boldsymbol{q}} = G(\boldsymbol{q})\boldsymbol{u}, \tag{2.1}$$

where $\boldsymbol{q} \in \mathbb{R}^k$ is the vector of generalized configuration coordinates of the system. The *Lagrangian* $\mathcal{L} = V_\mathrm{K} - V_\mathrm{P}$ equals the difference between the kinetic co-energy V_K and the potential energy V_P. The kinetic co-energy is explicitly given as $V_\mathrm{K} = \frac{1}{2}\dot{\boldsymbol{q}}^T M(\boldsymbol{q})\dot{\boldsymbol{q}}$, with a symmetric, positive definite inertia matrix $M(\boldsymbol{q}) \in \mathbb{R}^{k\times k}$. The generalized forces $\boldsymbol{u} \in \mathbb{R}^m$ act on the system with an input matrix $G(\boldsymbol{q}) \in \mathbb{R}^{k\times m}$. We define the generalized *momenta* for every Lagrangian $\boldsymbol{p} := \frac{\partial \mathcal{L}}{\partial \dot{\boldsymbol{q}}}$ and obtain $\boldsymbol{p} = M(\boldsymbol{q})\dot{\boldsymbol{q}}$. Introducing the *Hamiltonian* (energy) function $\mathcal{H}(\boldsymbol{q}, \boldsymbol{p}) = \boldsymbol{p}^T\dot{\boldsymbol{q}} - \mathcal{L}(\boldsymbol{q}, \dot{\boldsymbol{q}})$ we can rewrite the Euler-Lagrange equation in form of the classical Hamiltonian

equations of a mechanical system

$$\begin{aligned}\dot{\boldsymbol{q}} &= \frac{\partial \mathcal{H}}{\partial \boldsymbol{p}}(\boldsymbol{q},\boldsymbol{p}) \\ \dot{\boldsymbol{p}} &= -\frac{\partial \mathcal{H}}{\partial \boldsymbol{q}}(\boldsymbol{q},\boldsymbol{p}) + G(\boldsymbol{q})\boldsymbol{u}\end{aligned} \tag{2.2}$$

The Hamiltonian describes the total energy stored in the system [vdS06], thus the energy balance is

$$\frac{d}{dt}\mathcal{H} = \frac{\partial^T \mathcal{H}}{\partial \boldsymbol{q}}(\boldsymbol{q},\boldsymbol{p})\dot{\boldsymbol{q}} + \frac{\partial^T \mathcal{H}}{\partial p}(\boldsymbol{q},\boldsymbol{p})\dot{\boldsymbol{p}} = \boldsymbol{u}^T G^T(\boldsymbol{q})\dot{\boldsymbol{q}} = \boldsymbol{u}^T\boldsymbol{y} \tag{2.3}$$

Hamiltonian systems are energy conservative, i.e. the energy supplied through the port is stored in the system. In the upper equation a new output $\boldsymbol{y} = G^T(\boldsymbol{q})\dot{\boldsymbol{q}}$ is introduced. Clearly the product $\boldsymbol{y}^T\boldsymbol{u}$ is the exchanged power and we call the pair $(\boldsymbol{u},\boldsymbol{y})$ a *power port*. The general equations of a port-Hamiltonian system are

$$\begin{aligned}\dot{\boldsymbol{q}} &= \frac{\partial \mathcal{H}}{\partial \boldsymbol{p}}(\boldsymbol{q},\boldsymbol{p}) \\ \dot{\boldsymbol{p}} &= -\frac{\partial \mathcal{H}}{\partial \boldsymbol{q}}(\boldsymbol{q},\boldsymbol{p}) + G(\boldsymbol{q})\boldsymbol{u} \\ \boldsymbol{y} &= G^T(\boldsymbol{q})\frac{\partial \mathcal{H}}{\partial \boldsymbol{p}}(\boldsymbol{q},\boldsymbol{p})\end{aligned} \tag{2.4}$$

Port-Hamiltonian systems are suitable to describe a variety of physical systems including mechanical, electrical, thermal and hydraulic elements, see [DMSB09] for an overview. The common ground is that inputs and outputs are dual quantities, this motivates the more general input-output concept of flows $\boldsymbol{u}$ and efforts $\boldsymbol{y}$ forming the port variables $(\boldsymbol{u},\boldsymbol{y})$.

Example 2.1:

Consider a simple one-dimensional spring-mass system described by the equation $m\ddot{x} = -kx + F$ and shown in figure 2.1. The parameters m, k, F denote the mass, stiffness and external force acting on the mass respectively. A state space formulation of the system is

$$\begin{pmatrix}\dot{x}\\ \ddot{x}\end{pmatrix} = \begin{pmatrix}0 & 1\\ -\frac{k}{m} & 0\end{pmatrix}\begin{pmatrix}x\\ \dot{x}\end{pmatrix} + \begin{pmatrix}0\\ 1\end{pmatrix}\frac{F}{m} \tag{2.5}$$

In the Hamiltonian approach the system is described based on the energy functions, being $V_{\mathrm{P}}(q) = \frac{1}{2}kq^2$ for the spring and $V_{\mathrm{K}}(p) = \frac{1}{2m}p^2$ for the mass. The total energy

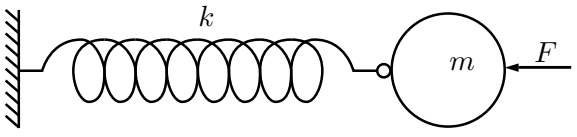

Figure 2.1: Spring-mass example

Table 2.1: port-Hamiltonian system variables of mechanical elements

	Spring	**Mass**	**Damper**
Effort variable	Force F	Velocity $\dot{x}$	Force F
Flow variable	Velocity $\dot{x}$	Force $F = \dot{p}$	Velocity $\dot{x}$
State variable	Position x	Momentum p	-
Energy function	$E(x) = \frac{1}{2}kx^2$	$E(p) = \frac{p^2}{2m}$	$E(\dot{x}) = D\dot{x}^2$ (diss. co-energy)

is thus the Hamiltonian $\mathcal{H}(q,p) = V_\mathrm{K} + V_\mathrm{P}$ The state variables are thus replaced by the energy states, the *configuration* $q = x$ accounting for the spring and the *momentum* $p = m\dot{x}$ accounting for the mass.

$$\begin{aligned} \begin{pmatrix} \dot{q} \\ \dot{p} \end{pmatrix} &= \begin{pmatrix} 0 & 1 \\ -1 & 0 \end{pmatrix} \begin{pmatrix} \frac{\partial \mathcal{H}}{\partial q}(q,p) \\ \frac{\partial \mathcal{H}}{\partial p}(q,p) \end{pmatrix} + \begin{pmatrix} 0 \\ 1 \end{pmatrix} F \\ y &= \begin{pmatrix} 0 & 1 \end{pmatrix} \begin{pmatrix} \frac{\partial \mathcal{H}}{\partial q}(q,p) \\ \frac{\partial \mathcal{H}}{\partial p}(q,p) \end{pmatrix} \end{aligned} \tag{2.6}$$

Key aspect of port-Hamiltonian system is the division into atomic energy storing elements (spring, mass) and their proper interconnection. In the example we have implicitly done this by defining energy functions and states for both elements. The rules of interconnection are explicitly given by:

- equal velocity of a spring tip and the mass $\dot{x} = \frac{\partial \mathcal{H}}{\partial p}$(rigid connection)
- opposite forces at the spring tip and the mass $\dot{p} = -\frac{\partial \mathcal{H}}{\partial q} + F$ (principle of action-reaction)

Due to the *second law of thermodynamics* real mechanical systems are never energy conservative. Thus we require energy dissipating elements (since thermal energy is "lost" w.r.t. the mechanical domain). A mechanical system is then described by its basic elements: springs, masses and dampers. Table 2.1 gives an overview of the elements and their characterizing quantities. Note that dissipation elements do not have a state because they do not store energy. It is worth pointing out that the *flows* are the time derivatives of the *states*.
Next to *energy-storing* and *-dissipating* there is a third class of elements, namely *energy-conservative* structures. Elements within this group are transformers, gyrators and ideal constraints. They are used to redirect the power flow in the system. It is possible to merge all *energy-storing* elements into a single object representation (see Fig. 2.2). Analogously this can be done for the dissipation elements. The interconnecting structure (denoted by $\mathcal{D}$ in Fig. 2.2), consisting of the *energy-conservative* elements, formalizes the energy routing and geometric dependencies of the system. A detailed explanation is given in the next subsection.

Complex physical systems can be modelled as a network of energy storing and dissipating elements, similar an electrical network consisting of resistors, inductors and capacitors. The rules of interconnection are Newton's third law (action-reaction), Kirchhoff's laws and power-conserving elements like transformers or gyrators. The aim of port-Hamiltonian modelling is to describe the power-conserving elements with the interconnection laws as a geometric structure and to define the Hamiltonian function as the total energy of the system.
The power flowing between the system's portions is described by a general set of flows $\boldsymbol{f}$ and efforts $\boldsymbol{e}$, forming the product $\boldsymbol{e}^T\boldsymbol{f}$.

2.2.1 Dirac structures and interconnection ports

The energy-routing structure forms the basis of every port-Hamiltonian system. It can be compared to the printed circuit board in electronics, where capacitors, inductors and resistors are the energy-storing and damping elements. Mathematically it has the form of a *Dirac* structure [vdS06]. The main property of a Dirac structure is power conservation, i.e. the power flowing into and out of it always sums to zero. We can define the set of ports $(\boldsymbol{f}, \boldsymbol{e})$ connecting to the Dirac structure $\mathcal{D}$, thus

$$\boldsymbol{e}^T\boldsymbol{f} = 0 \;\; \forall(\boldsymbol{f}, \boldsymbol{e}) \in \mathcal{D} \tag{2.7}$$

Where $\mathcal{D}$ is a subspace of the space of flow and effort $\mathcal{D} \subset \mathcal{E} \times \mathcal{F}$. The space of flows is $\boldsymbol{f} \in \mathcal{F}$, the space of efforts is its dual linear space $\boldsymbol{e} \in \mathcal{E} = \mathcal{F}^*$. The Dirac structure has the same dimension than the space of flows $dim\mathcal{D} = dim\mathcal{F}$. Further mathematical requirements can be found in literature [vdS06, vdSJ14].
Power conservation means that supplied energy is either stored or dissipated in the system. All storing and resistive elements can be represented each in a single element as shown in figure 2.2. Three ports join in the interconnection structure, one for external supply $(\boldsymbol{u}, \boldsymbol{y})$, one for the sum of storing elements $(\boldsymbol{f}_\mathrm{S}, \boldsymbol{e}_\mathrm{S})$ and one for the resistive elements $(\boldsymbol{f}_R, \boldsymbol{e}_R)$. Mathematically the interconnection of ports is defined by the Dirac structure matrix D

$$\begin{pmatrix} \boldsymbol{y} \\ \boldsymbol{f}_\mathrm{S} \\ \boldsymbol{e}_\mathrm{R} \end{pmatrix} = D \begin{pmatrix} \boldsymbol{u} \\ \boldsymbol{e}_\mathrm{S} \\ \boldsymbol{f}_\mathrm{R} \end{pmatrix} \tag{2.8}$$

It can be shown that for a skew-symmetric D the power balance of the ports is

$$\boldsymbol{e}_\mathrm{S}{}^T\boldsymbol{f}_\mathrm{S} + \boldsymbol{y}^T\boldsymbol{u} + \boldsymbol{e}_\mathrm{R}{}^T\boldsymbol{f}_\mathrm{R} = 0, \tag{2.9}$$

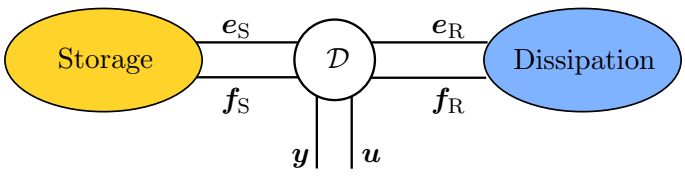

Figure 2.2: port-Hamiltonian system structure

This fulfils the desired power conservation.
We can simplify equation 2.2 by setting $\boldsymbol{x} = (\boldsymbol{q}^T, \boldsymbol{p}^T)^T$ and introduce a general port-Hamiltonian system of the form

$$\begin{aligned} \dot{\boldsymbol{x}} &= [J(\boldsymbol{x}) - R(\boldsymbol{x})]\frac{\partial \mathcal{H}}{\partial \boldsymbol{x}}(\boldsymbol{x}) + G(\boldsymbol{x})\boldsymbol{u} \\ \boldsymbol{y} &= G^T(\boldsymbol{x})\frac{\partial \mathcal{H}}{\partial \boldsymbol{x}}(\boldsymbol{x}), \end{aligned} \tag{2.10}$$

with $J(\boldsymbol{x}) \in \mathbb{R}^{2k\times 2k}$ being a skew-symmetric structure matrix and $R(\boldsymbol{x}) \in \mathbb{R}^{2k\times 2k}$ being a positive semi-definite, symmetric dissipation matrix.

Energy storage port

The port accounts for the internal storage of the system, its port variables are $(\boldsymbol{f}_\mathrm{S}, \boldsymbol{e}_\mathrm{S})$. The power supplied through this port is stored in the Hamiltonian energy function $\mathcal{H}(\boldsymbol{x})$ of the system. The resulting energy balance is:

$$\frac{d}{dt}\mathcal{H} = \frac{\partial^T \mathcal{H}}{\partial \boldsymbol{x}}(\boldsymbol{x})\dot{\boldsymbol{x}} \tag{2.11}$$

The flow variable is the energy rate $\boldsymbol{f}_\mathrm{S} = -\dot{\boldsymbol{x}}$ and the effort variable is $\boldsymbol{e}_\mathrm{S} = \frac{\partial \mathcal{H}}{\partial \boldsymbol{x}}(\boldsymbol{x})$.

Energy dissipation port

The port corresponds to internal dissipation and can be used to model resistive elements. The port variables are described by the general resistive relation

$$F(\boldsymbol{f}_\mathrm{R}, \boldsymbol{e}_\mathrm{R}) = 0 \tag{2.12}$$

with the property ${\boldsymbol{e}_\mathrm{R}}^T \boldsymbol{f}_\mathrm{R} \leq 0$ (energy dissipation). An important special case is the input-output resistive relation $\boldsymbol{f}_\mathrm{R} = -F(\boldsymbol{e}_\mathrm{R})$, for linear elements simply

$$\boldsymbol{f}_\mathrm{R} = -R\boldsymbol{e}_\mathrm{R}\ ,\ R = R^T \succeq 0 \tag{2.13}$$

For an uncontrolled system that does not interact with the environment, i.e. no energy exchange through the external port, the energy balance is:

$$\frac{d\mathcal{H}}{dt} = -{\boldsymbol{e}_\mathrm{S}}^T \boldsymbol{f}_\mathrm{S} = {\boldsymbol{e}_\mathrm{R}}^T \boldsymbol{f}_\mathrm{R} \leq 0 \tag{2.14}$$

External port

The external port $(\boldsymbol{u}, \boldsymbol{y})$ can be further split into an environment *interaction* $(\boldsymbol{f}^\mathrm{I}, \boldsymbol{e}^\mathrm{I})$ and a *control* port $(\boldsymbol{f}_\mathrm{C}, \boldsymbol{e}_\mathrm{C})$, satisfying $\boldsymbol{y}^T\boldsymbol{u} = {\boldsymbol{e}_\mathrm{I}}^T \boldsymbol{f}_\mathrm{I} + {\boldsymbol{e}_\mathrm{C}}^T \boldsymbol{f}_\mathrm{C}$. The power balance of the whole system then is

$${\boldsymbol{e}_\mathrm{S}}^T \boldsymbol{f}_\mathrm{S} + {\boldsymbol{e}_\mathrm{R}}^T \boldsymbol{f}_\mathrm{R} + {\boldsymbol{e}_\mathrm{I}}^T \boldsymbol{f}_\mathrm{I} + {\boldsymbol{e}_\mathrm{C}}^T \boldsymbol{f}_\mathrm{C} = 0 \tag{2.15}$$

or by using (2.11)

$$\frac{d\mathcal{H}}{dt} = {\boldsymbol{e}_\mathrm{R}}^T \boldsymbol{f}_\mathrm{R} + {\boldsymbol{e}_\mathrm{I}}^T \boldsymbol{f}_\mathrm{I} + {\boldsymbol{e}_\mathrm{C}}^T \boldsymbol{f}_\mathrm{C} \tag{2.16}$$

2.2.2 Interconnection of port-Hamiltonian systems

It is important to notice that the interconnection of two port-Hamiltonian systems is again a port-Hamiltonian system [vdSJ14]. Consider two general systems ($i = 1, 2$) with open control and environment interaction ports:

$$\begin{aligned} \dot{\boldsymbol{x}}_i &= (J_i - R_i)\frac{\partial \mathcal{H}_i}{\partial \boldsymbol{x}_i} + \begin{pmatrix} G_{\mathrm{C},i} & G_{\mathrm{I},i} \end{pmatrix} \begin{pmatrix} \boldsymbol{f}_{\mathrm{C},i} \\ \boldsymbol{f}_{\mathrm{I},i} \end{pmatrix} \\ \begin{pmatrix} \boldsymbol{e}_{\mathrm{C},i} \\ \boldsymbol{e}_{\mathrm{I},i} \end{pmatrix} &= \begin{pmatrix} G_{\mathrm{C},i}^T \\ G_{\mathrm{I},i}^T \end{pmatrix} \frac{\partial \mathcal{H}_i}{\partial \boldsymbol{x}_i} \end{aligned} \tag{2.17}$$

where J_i, R_i are a skew-symmetric structure matrix and a positive semi-definite symmetric dissipation matrix. The input matrices $G_{\mathrm{C},i}$, $G_{\mathrm{I},i}$ describe the effect of a control action and the environment interaction respectively. For notational convenience the usual dependencies on the states are omitted.
The control inputs and outputs are now connected by setting $\boldsymbol{f}_{\mathrm{C},1} = \boldsymbol{e}_{\mathrm{C},2}$ and $\boldsymbol{f}_{\mathrm{C},2} = -\boldsymbol{e}_{\mathrm{C},1}$. Note that the minus sign is necessary for power conservation. The power exchanged by the i-th system is $P_i = {\boldsymbol{e}_{\mathrm{C},i}}^T \boldsymbol{f}_{\mathrm{C},i}$, therefore the total exchanged energy fulfils $P_1 + P_2 = 0$. The resulting interconnected system still has the environment interaction ports open:

$$\begin{aligned} \dot{\boldsymbol{x}} &= (J - R)\frac{\partial \mathcal{H}}{\partial \boldsymbol{x}} + \begin{pmatrix} G_{\mathrm{I},1} & G_{\mathrm{I},2} \end{pmatrix} \begin{pmatrix} \boldsymbol{f}_{\mathrm{C},1} \\ \boldsymbol{f}_{\mathrm{I},2} \end{pmatrix} \\ \begin{pmatrix} \boldsymbol{e}_{\mathrm{I},1} \\ \boldsymbol{e}_{\mathrm{I},2} \end{pmatrix} &= \begin{pmatrix} G_{\mathrm{I},1}^T \\ G_{\mathrm{I},2}^T \end{pmatrix} \frac{\partial \mathcal{H}}{\partial \boldsymbol{x}} \end{aligned} \tag{2.18}$$

where $\boldsymbol{x} = (\boldsymbol{x}_1^T, \boldsymbol{x}_2^T)^T$ and $\mathcal{H} = \mathcal{H}_1 + \mathcal{H}_2$ is the sum of the two energies. The structure and dissipation matrix become:

$$J = \begin{pmatrix} J_1 & G_{\mathrm{C},1} G_{\mathrm{C},2}^T \\ -G_{\mathrm{C},2} G_{\mathrm{C},1}^T & J_2 \end{pmatrix}, \; R = \begin{pmatrix} R_1 & 0 \\ 0 & R_2 \end{pmatrix}$$

2.2.3 port-Hamiltonian systems and passivity

A system is *passive* if there exists a differentiable storage function $\mathcal{H}(\boldsymbol{x}) \geq 0$ that satisfies

$$\frac{d}{dt}\mathcal{H}(\boldsymbol{x}(t)) \leq \boldsymbol{u}^T(t)\boldsymbol{y}(t) \tag{2.19}$$

The product of the input-output pair $(\boldsymbol{u}, \boldsymbol{y})$ is the supplied power. By definition the Hamiltonian function represents the total energy stored in the system. For a

port-Hamiltonian system of the form of equation (2.10) we have

$$\begin{aligned}\frac{d}{dt}\mathcal{H}(\boldsymbol{x}) &= \frac{\partial^T\mathcal{H}}{\partial\boldsymbol{x}}\frac{d\boldsymbol{x}}{dt} = \frac{\partial^T\mathcal{H}}{\partial\boldsymbol{x}}\left[(J(\boldsymbol{x})-R(\boldsymbol{x}))\frac{\partial\mathcal{H}}{\partial\boldsymbol{x}}+G(\boldsymbol{x})\boldsymbol{u}\right]\\ &= \frac{\partial^T\mathcal{H}}{\partial\boldsymbol{x}}J(\boldsymbol{x})\frac{\partial\mathcal{H}}{\partial\boldsymbol{x}} - \frac{\partial^T\mathcal{H}}{\partial\boldsymbol{x}}R(\boldsymbol{x})\frac{\partial\mathcal{H}}{\partial\boldsymbol{x}} + (G^{-T}(\boldsymbol{x})e)^TG(\boldsymbol{x})\boldsymbol{u}\\ &= \boldsymbol{y}^T\boldsymbol{u} - \frac{\partial^T\mathcal{H}}{\partial\boldsymbol{x}}R(\boldsymbol{x})\frac{\partial\mathcal{H}}{\partial\boldsymbol{x}}\end{aligned} \tag{2.20}$$

The property $\frac{\partial^T\mathcal{H}}{\partial\boldsymbol{x}}J(\boldsymbol{x})\frac{\partial\mathcal{H}}{\partial\boldsymbol{x}} = 0$ holds for a skew symmetric matrix $J(\boldsymbol{x}) = -J(\boldsymbol{x})^T$. The product of the effort-flow pair $\boldsymbol{e}^T\boldsymbol{f}$ is the power supplied to the system. Since $R(\boldsymbol{x}) = R(\boldsymbol{x})^T \succeq 0$ is symmetric and positive semi-definite, we have $\frac{\partial^T\mathcal{H}}{\partial\boldsymbol{x}}R(\boldsymbol{x})\frac{\partial\mathcal{H}}{\partial\boldsymbol{x}} \geq 0$. Conclusively equation (2.19) holds for every port-Hamiltonian system that satisfies the properties of equation (2.10), clearly the system is *passive*. If $R = 0$, i.e. the system exhibits no dissipation we call it *lossless*.
Passivity is a sufficient criterion for asymptotic stability [OvdSMM01].

2.3 3D-space modelling of mechanical systems

2.3.1 Euclidean space and motions

Coordinate frames

A coordinate frame of the three-dimensional Euclidean space is a 4-tuple of the form $\Psi = (\boldsymbol{o}, \hat{\boldsymbol{x}}, \hat{\boldsymbol{y}}, \hat{\boldsymbol{z}})$. Where $\boldsymbol{o}$ is the three-dimensional vector of the origin and $\hat{\boldsymbol{x}}, \hat{\boldsymbol{y}}, \hat{\boldsymbol{z}}$ are the linear independent, orthonormal coordinate vectors. Consider two coordinate frames Ψ_1, Ψ_2 which share the same origin but differ in orientation due to different choices of $\hat{\boldsymbol{x}}_i, \hat{\boldsymbol{y}}_i, \hat{\boldsymbol{z}}_i,\ i = 1, 2$. The change of orientation from Ψ_i to Ψ_j is described by the rotation matrix R_i^j. The set of rotation matrices is called *special orthonormal* group ($SO(3)$) [Str01a] and is defined as:

$$SO(3) = \{\mathrm{R} \in \mathbb{R}^{3\times3} \mid \mathrm{R}^{-1} = \mathrm{R}^T, det\mathrm{R} = 1\} \tag{2.21}$$

Usually coordinate frames are defined with respect to an inertial frame, and the coordinate vectors $\hat{\boldsymbol{x}}, \hat{\boldsymbol{y}}, \hat{\boldsymbol{z}}$ are chosen equal for all frames, deviations of orientation are represented by a rotation matrix relative to the inertial frame. In general a change of coordinate frames from Ψ_i to Ψ_j can be expressed with the homogeneous matrix

$$H_i^j := \begin{pmatrix}\mathrm{R}_i^j & \boldsymbol{p}_i^j\\ 0_{1\times3} & 1\end{pmatrix}$$

where $\boldsymbol{p}_i^j = \boldsymbol{o}_j - \boldsymbol{o}_i$ denotes the distance between the origins. A point $\boldsymbol{p}^i \in \mathbb{R}^3$ expressed in Ψ_i is cast into Ψ_j by

$$\begin{pmatrix}\boldsymbol{p}^j\\ 1\end{pmatrix} = H_i^j\begin{pmatrix}\boldsymbol{p}^i\\ 1\end{pmatrix} \tag{2.22}$$

. The inverse transformation H_j^i is given by

$$H_i^j = (H_i^j)^{-1} = \begin{pmatrix} (\mathrm{R}_i^j)^T & -(\mathrm{R}_i^j)^T \boldsymbol{p}_i^j \\ 0_{1\times 3} & 1 \end{pmatrix}$$

and is still a homogeneous matrix. The set of homogeneous matrices is called the *special Euclidean* group:

$$SE(3) := \{ \begin{pmatrix} \mathrm{R} & \boldsymbol{p} \\ 0 & 1 \end{pmatrix} \mid \mathrm{R} \in SO(3), \boldsymbol{p} \in \mathbb{R}^3 \} \tag{2.23}$$

The $SE(3)$ is a matrix Lie group, composed of the set of homogeneous matrices H_i^j and the matrix multiplication being the group operation. For more information on Lie groups see e.g. [Str01b].

Twists and wrenches

Consider any point $\boldsymbol{p}$ not moving in coordinate frames Ψ_i, i.e. $\dot{\boldsymbol{p}}^i = 0$. If $\boldsymbol{p}$ is moving in another coordinate frame Ψ_j, the two frame move with respect to each other. The trajectory can be described as a function of time: $H_i^j(t) \in SE(3)$. By differentiating (2.22) one obtains

$$\begin{pmatrix} \dot{\boldsymbol{p}}^j(t) \\ 1 \end{pmatrix} = \dot{H}_i^j(t) \begin{pmatrix} \boldsymbol{p}^i \\ 1 \end{pmatrix}$$

$\dot{H}_i^j$ describes both motion and a change of the reference frame. A separated representation is

$$\begin{pmatrix} \dot{\boldsymbol{p}}^j(t) \\ 1 \end{pmatrix} = \tilde{T}_i^{j,j} \left(H_i^j \begin{pmatrix} \boldsymbol{p}^i \\ 1 \end{pmatrix} \right) \tag{2.24}$$

$\dot{H}_i^j$ is a tangential vector along the trajectory $H_i^j(t)$ and thus in the tangent space of the $SE(3)$: $\dot{H}_i^j \in T_{H_i^j} SE(3)$. To obtain a representation of motion which is referenced to a coordinate frame, we can map $\dot{H}_i^j$ to the identity of the $SE(3)$. At the identity e of the $SE(3)$ the tangent space $T_e SE(3)$ has the structure of a Lie algebra. The Lie algebra of the $SE(3)$ is denoted by $\mathfrak{se}(3)$. This is done either by left or right translation, for a definition see [Str01b]. The right translation is used in (2.24) and is written compactly

$$\dot{H}_i^j = \tilde{T}_i^{j,j} H_i^j \tag{2.25}$$

The left translation leads to

$$\dot{H}_i^j = H_i^j \tilde{T}_i^{i,j} \tag{2.26}$$

We call $\tilde{T} \in T_e SE(3)$ a twist and the $\mathfrak{se}(3)$ the space of twists. Let us look more closely at this representation by calculating the twist from the elements of the homogeneous matrix

$$
\begin{aligned}
T_i^j = \dot{H}_i^j H_j^i &= \begin{pmatrix} \dot{\mathrm{R}}_i^j & \dot{\boldsymbol{p}}_i^j \\ 0 & 0 \end{pmatrix} \begin{pmatrix} \mathrm{R}_j^i & \boldsymbol{p}_j^i \\ 0 & 1 \end{pmatrix} = \begin{pmatrix} \dot{\mathrm{R}}_i^j & \dot{\boldsymbol{p}}_i^j \\ 0 & 0 \end{pmatrix} \begin{pmatrix} (\mathrm{R}_i^j)^T & -(\mathrm{R}_i^j)^T \boldsymbol{p}_i^j \\ 0 & 1 \end{pmatrix} \\
&= \begin{pmatrix} \dot{\mathrm{R}}_i^j (\mathrm{R}_i^j)^T & -\dot{\mathrm{R}}_i^j (\mathrm{R}_i^j)^T \boldsymbol{p}_i^j + \dot{\boldsymbol{p}}_i^j \\ 0 & 0 \end{pmatrix} =: \begin{pmatrix} \tilde{\omega}_i^j & \boldsymbol{v}_i^j \\ 0 & 0 \end{pmatrix}
\end{aligned} \tag{2.27}
$$

It is clear from this equation that the linear velocity part $\boldsymbol{v}_i^j$ is not the velocity of the frame Ψ_i with respect to Ψ_j, identified by $\dot{\boldsymbol{p}}_i^j$. This twist representation is described by the *screw theory* (see e.g. [WS08]). It can be visualized by the angular velocity around an axis and the linear velocity along this axis.
Next to the 4×4 matrix $\tilde{T}$ there exists also a vector representation $T \in \mathbb{R}^6$

$$
\tilde{T} = \begin{pmatrix} \tilde{\omega} & \boldsymbol{v} \\ 0 & 0 \end{pmatrix} \ , \ T = \begin{pmatrix} \boldsymbol{\omega} \\ \boldsymbol{v} \end{pmatrix} \tag{2.28}
$$

wherein $\boldsymbol{v} \in \mathbb{R}^3$ is the linear velocity and $\boldsymbol{\omega} \in \mathbb{R}^3$ is the angular velocity. $\tilde{\omega} \in \mathbb{R}^{3\times 3}$ is the skew-symmetric representation of the vector $\boldsymbol{\omega}$

$$
\boldsymbol{\omega} = \begin{pmatrix} \omega_1 \\ \omega_2 \\ \omega_3 \end{pmatrix} \ \Rightarrow \ \tilde{\omega} = \begin{pmatrix} 0 & -\omega_3 & \omega_2 \\ \omega_3 & 0 & \omega_1 \\ -\omega_2 & \omega_1 & 0 \end{pmatrix} \tag{2.29}
$$

Left and right translations lead to different representations of a twist:

- $T_i^{k,j}$ is the twist of Ψ_i with respect to Ψ_j expressed in the frame Ψ_k
- $T_i^j = T_i^{j,j}$ is the twist of Ψ_i with respect to Ψ_j expressed naturally in Ψ_j

Changes of coordinates for twists are of the form

$$
\tilde{T}_i^{j,j} = \tilde{T}_i^j = H_i^j \tilde{T}_i^{i,j} H_j^i \tag{2.30}
$$

or for the vector representation

$$
T_i^j = Ad_{H_i^j} T_i^{i,j} \ , \ Ad_{H_i^j} = \begin{pmatrix} R_i^j & 0 \\ \tilde{p}_i^j R_i^j & R_i^j \end{pmatrix} \tag{2.31}
$$

The dual vector space of $\mathfrak{se}(3)$ is the space of linear operations from $\mathfrak{se}(3)$ to $\mathbb{R}$. It is denoted by $\mathfrak{se}^*(3)$ and represents the space of wrenches W. Wrenches decompose to moments $\boldsymbol{m} \in \mathbb{R}^3$ and forces $\mathbf{f} \in \mathbb{R}^3 \in \mathbb{R}^3$.

$$
W = (\boldsymbol{m} \ \ \mathbf{f}) \ , \ \tilde{W} = \begin{pmatrix} \tilde{m} & \mathbf{f} \\ 0 & 0 \end{pmatrix} \tag{2.32}
$$

Again $\tilde{W} \in \mathbb{R}^{4\times4}$ is a matrix while $W \in \mathbb{R}^6$ is the row vector representation. The change of coordinates for twists is similar to the case of twists:

$$(W_i^{k,i})^T = Ad_{H_k^i}^T (W_i^i)^T \tag{2.33}$$

Here the mapping is in the opposite direction, from Ψ_j to Ψ_i, what is a consequence of the fact that wrenches are duals to twists. Again there are different representations of wrenches:

- $W_i^{k,j}$ is the wrench applied to a spring connecting Ψ_i to Ψ_j on the side of Ψ_i expressed in the coordinate frame Ψ_k.
- W_i^k is the wrench applied to a body attached to Ψ_i expressed in the coordinate frame Ψ_k.

These definitions lead to the following rules of interconnection: Connecting a body and spring in the point Ψ_i and applying the principle of action and reaction we get $W_i^{k,j} = -W_i^k$. Due to the nodicity of a spring we have $W_i^{k,j} = -W_j^{k,i}$

We define power flowing through a port by the duality product of flow and effort, in the mechanical domain this twist and wrench. On a vector space level the power port $\mathcal{P}$ is defined by the Cartesian product of the Lie algebra $\mathfrak{se}(3)$ and its dual $\mathfrak{se}^*(3)$: $\mathcal{P} = \mathfrak{se}(3) \times \mathfrak{se}^*(3)$.

2.3.2 Input-state-output port-Hamiltonian systems in 3D space

The simple relation, between the time-derivative of the configuration and the change of kinetic energy, $\frac{\partial \mathcal{H}}{\partial \boldsymbol{p}} = \dot{\boldsymbol{q}}$ does not hold for a 3D-mechanical system. It is detailed in the next subsection that $\frac{\partial \mathcal{H}}{\partial P_i^i} = T_i^{i,0} = H_0^i \dot{H}_i^0$, with the H_0^i being the configuration variable and P_i^i the momentum. Thus the interconnecting Dirac structure depends on the configuration H_0^i and we call it a *modulated* Dirac structure. Mathematically the state space of the system is then a *manifold*, for details see [vdSJ14]. We define local coordinates $\boldsymbol{x}$ on the state manifold $\mathcal{X}$, associate the flows towards the energy storage with $\boldsymbol{f}_\mathrm{S} = -\dot{\boldsymbol{x}}$ and the efforts with $\boldsymbol{e}_\mathrm{S} = \frac{\partial V}{\partial \boldsymbol{x}}$. The flows are elements of the tangent space $T_x\mathcal{X}$ of the state manifold at the state $\boldsymbol{x} \in \mathcal{X}$ and the efforts are elements of the co-tangent space $T_x^*\mathcal{X}$. The resulting port-Hamiltonian system in 3D space is of the form

$$\begin{aligned} \dot{\boldsymbol{x}} &= [J(\boldsymbol{x}) - R(\boldsymbol{x})] \frac{\partial \mathcal{H}}{\partial \boldsymbol{x}}(\boldsymbol{x}) + G(\boldsymbol{x})\boldsymbol{u} \\ \boldsymbol{y} &= G^T(\boldsymbol{x}) \frac{\partial \mathcal{H}}{\partial \boldsymbol{x}} \end{aligned} \tag{2.34}$$

with a skew-symmetric matrix $J(\boldsymbol{x})$ and a resistive structure matrix $R(\boldsymbol{x})$ which is symmetric and positive semi-definite. Clearly $\boldsymbol{u}$ and $\boldsymbol{y}$ denote the input and

output respectively and this representation is again of the *input-state-output* form. In the following section we introduce the corresponding representations of atomic mechanical elements.

2.3.3 Dynamics of physical components

Springs

A *spring* is the ideal, lossless element storing potential energy. It is connected to two bodies and is defined by a potential energy function. The energy is a function of the relative displacement of the attached bodies. Consider a spring between the two bodies B_i and B_j, with coordinate frames Ψ_i and Ψ_j fixed to the respective body. The stored potential energy is positive definite function of the form

$$V_{\mathrm{P}} : SE(3) \to \mathbb{R};\ H_i^j \mapsto V_{\mathrm{P}}(H_i^j) \tag{2.35}$$

For explicit energy functions for different types of springs see [Str01b]. The input-state-output form is defined by the relative displacement H_i^j (state variable), the wrench $W_i^{j,j}$ (effort) and the twist T_i^j (flow).

$$\begin{aligned} \dot{H}_i^j &= T_i^j H_i^j \\ W_i^{j,j} &= \frac{\partial V_{\mathrm{P}}(H_i^j)}{\partial H_i^j}(H_i^j)^T \end{aligned} \tag{2.36}$$

Note that V_{P} is an energetic minimum when H_i^j is the identity matrix I_4. An energetic minimum is physically necessary, otherwise infinite energy would be extractable from the spring. With $H_i^j = I_4$ the frames Ψ_i and Ψ_j coincide. It is possible to define springs with non-zero rest-length by introducing coordinate frames Ψ_{ic} and Ψ_{jc} rigidly attached to Ψ_i and Ψ_j respectively. The spring is now between the new frames, thus the energetic minimum is $H_{ic}^{jc} = I_4$. The displacements H_i^{ic}, H_j^{jc} are the resulting rest-lengths. Frames Ψ_{ic} and Ψ_{jc} can be chosen to represent the *center of stiffness*, where translation and rotation are maximally decoupled [SMA99].

Inertias

Inertias are special since they in general store two types of energy: kinetic and potential energy due to gravitation. At first we exclude the gravitational terms and focus on motion. Kinetic energy is a function of the relative motion w.r.t. an inertial reference. When expressing motion in non-inertial or accelerated reference frames, fictitious forces such as the *Coriolis* or the *centrifugal* force need to be considered. Let us start from *Newton's* second law of dynamics, the time derivative of a body's momentum is equal to the applied wrench.

$$\dot{P}_b^0 = W_b^0 \tag{2.37}$$

The momentum of the inertia b and the wrench acting on it are both expressed in the inertial reference frame Ψ_0. Let us consider the non-inertial frame Ψ_b, fixed to the inertia. We start by changing coordinates, clearly we have $W_b^0 = Ad_{H_0^b}^T W_b^b$. It is detailed in [Str01b] that $P_0^b \in \mathfrak{se}^*(3)$ and thus the same transformation as for wrenches applies $P_b^0 = Ad_{H_0^b}^T P_b^b$. Expressing the *Newton's* second law in the non-inertial frame Ψ_b we have

$$\frac{d}{dt}(Ad_{H_0^b}^T P_b^b) = Ad_{H_0^b}^T W_b^b \tag{2.38}$$

The evolution of the accelerated body frame Ψ_b w.r.t to the inertial frame is time dependent. The time derivative of the transformation is $\frac{d}{dt}Ad_{H_0^b}^T = -Ad_{H_0^b}^T ad_{T_b^{b,0}}^T$, with the *adjoint* representation (see for example [Str01a]):

$$ad_{T_b^{b,0}}^T = \begin{pmatrix} -\tilde{\omega}_b^{b,0} & -\tilde{v}_b^{b,0} \\ 0 & -\tilde{\omega}_b^{b,0} \end{pmatrix} \tag{2.39}$$

The second law of dynamics expressed in the body's frame is then

$$\begin{aligned} Ad_{H_0^b}^T \dot{P}_b^b - Ad_{H_0^b}^T ad_{T_b^{b,0}}^T P_b^b &= Ad_{H_0^b}^T W_b^b \\ \dot{P}_b^b &= ad_{T_b^{b,0}}^T P_b^b + W_b^b \end{aligned} \tag{2.40}$$

This formulation is split into its rotational and translational components, then we can exchange twist and momentum by the following operation

$$\begin{pmatrix} \dot{P}_{b,\omega}^b \\ \dot{P}_{b,v}^b \end{pmatrix} = \begin{pmatrix} -\tilde{\omega}_b^{b,0} & -\tilde{v}_b^{b,0} \\ 0 & -\tilde{\omega}_b^{b,0} \end{pmatrix} \begin{pmatrix} P_{b,\omega}^b \\ P_{b,v}^b \end{pmatrix} + W_b^b = \begin{pmatrix} \tilde{P}_{b,\omega}^b & \tilde{P}_{b,v}^b \\ \tilde{P}_{b,v}^b & 0 \end{pmatrix} \begin{pmatrix} \omega_b^{b,0} \\ v_b^{b,0} \end{pmatrix} + W_b^b \tag{2.41}$$

This clearly corresponds to the classical description of a rigid body's dynamics of the form

$$\dot{P}_b^b = M_b \dot{T}_b^{b,0} = C_b T_b^{b,0} + W_b^b \tag{2.42}$$

Here M_b describes the body's inertia and C_b accounts for Coriolis and centrifugal terms.

Towards port-Hamiltonian representation we start from the kinetic (co-)energy given by $V_{\mathrm{K}}^*(T_b^{b,0}) = \frac{1}{2}(T_b^{b,0})^T M_b T_b^{b,0}$. Formally speaking the kinetic energy is a function of the momentum. By using the relation of twist and momentum $P_b^b = M_b T_b^{b,0}$ we get the kinetic energy

$$V_{\mathrm{K}}(P_b^b) = \frac{1}{2}(P_b^b)^T M_b^{-1} P_b^b \tag{2.43}$$

By differentiating the kinetic energy w.r.t to the state variable P_b^b we obtain

$$\frac{\partial V_{\mathrm{K}}(P_b^b)}{\partial P_b^b} = M_b^{-1} P_b^b = T_b^{b,0} \tag{2.44}$$

Recall from Table 2.1 that the twist is the effort variable in the port-Hamiltonian representation of an inertia. The flow is the externally supplied wrench W_b^b, thus we obtain the port-Hamiltonian representation of a rigid body, neglecting gravity

$$\begin{aligned} \dot{P}_b^b &= C_b \frac{\partial V_{\mathrm{K}}(P_b^b)}{\partial P_b^b} + I_6 W_b^b \\ T_b^{b,0} &= I_6 \frac{\partial V_{\mathrm{K}}(P_b^b)}{\partial P_b^b} \end{aligned} \tag{2.45}$$

In cooperative manipulation we often deal with heavy objects, it is thus inevitable to include the potential energy resulting from the gravitational field. One can think of a spring connecting the body and an inertial frame associated with the ground. This spring can be formulated in port-Hamiltonian structure using the left translation (2.3.1)

$$\begin{aligned} \dot{H}_b^0 &= H_b^0 T_b^{b,0} \\ W_b^{b,0} &= (H_b^0)^T \frac{\partial V_{\mathrm{P}}(H_b^0)}{\partial H_b^0} \end{aligned} \tag{2.46}$$

Where V_g is a suitable energy function. For a combined description the potential and kinetic energy add up and we obtain the Hamiltonian $\mathcal{H}(P_b^b, H_b^0) = V_{\mathrm{K}}(P_b^b) + V_{\mathrm{P}}(H_b^0)$. Since there are two types of energy stored by *one* body, the twists in both energy systems are equal. The wrenches on the body add up

$$W_{kg}^b = W_b^b + C_b \frac{\partial \mathcal{H}(P_b^b, H_b^0)}{\partial P_b^b} - (H_b^0)^T \frac{\partial \mathcal{H}(P_b^b, H_b^0)}{\partial H_b^0}$$

Note that the negative sign in the upper equation comes from $W_b^b = -W_b^{b,0}$.
With this knowledge we can write the combined port-Hamiltonian representation

$$\begin{aligned} \begin{pmatrix} \dot{H}_b^0 \\ \dot{P}_b^b \end{pmatrix} &= \begin{pmatrix} 0 & H_b^0 \\ -(H_b^0)^T & C_b \end{pmatrix} \begin{pmatrix} \frac{\partial \mathcal{H}}{\partial H_b^0} \\ \frac{\partial \mathcal{H}}{\partial P_b^b} \end{pmatrix} + \begin{pmatrix} 0 \\ I_6 \end{pmatrix} W_b^b \\ T_b^{b,0} &= \begin{pmatrix} 0 & I_6 \end{pmatrix} \begin{pmatrix} \frac{\partial \mathcal{H}}{\partial H_b^0} \\ \frac{\partial \mathcal{H}}{\partial P_b^b} \end{pmatrix} \end{aligned} \tag{2.47}$$

Dampers

Dampers do not have a state since they do not store energy, they only dissipate it. Note that energy is not "destroyed" in the dampers but transformed into thermal energy. This can be modelled with a thermal port connected to the environment, for reasons of simplicity we discard the generated thermal energy. The easiest way to achieve damping is a linear resistive element R, such that the wrench is directly

proportional to twist. Consider for example a body's motion with respect to the inertial frame

$$W_b^b = RT_b^{b,0} \tag{2.48}$$

Or a damper in parallel with spring

$$W_i^{j,j} = RT_i^j \tag{2.49}$$

The dissipated co-energy is $E_d = \frac{1}{2}T^T RT$.

2.4 Spring-mass-damper systems in 3D space

Recall the motivating example from Section 2.2 of a simple spring-mass system. We can add a damper d to eq. (2.6)

$$\begin{pmatrix}\dot{q}\\ \dot{p}\end{pmatrix} = \begin{pmatrix}0 & 1\\ -1 & -d\end{pmatrix}\begin{pmatrix}\frac{\partial \mathcal{H}}{\partial q}(q,p)\\ \frac{\partial \mathcal{H}}{\partial p}(q,p)\end{pmatrix} + \begin{pmatrix}0\\ 1\end{pmatrix} F_e \tag{2.50}$$

This is the port-Hamiltonian representation of a one-dimensional spring-mass-damper system. Connecting two masses by a spring and a parallel damper is a simple model for a compliant contact [DS09]. Moreover spring-mass-damper systems are the basis of the virtual structures that form the controllers in section 2.6. In cooperative object manipulation there are two compliant contact situations. One to realize soft interaction between object and environment, i.e. actual and desired object position are impedance controlled (see also the related work section). The other is the object-manipulator connection. We start from the inertia subject to gravity (eq. (2.47) and add another spring to the body associated with Ψ_b. This spring connects to a desired object position assigned to Ψ_v. Its port-Hamiltonian representation is given by

$$\begin{aligned}\dot{H}_b^v &= H_b^v T_b^{b,v}\\ W_b^{b,v} &= (H_b^v)^T \frac{\partial V_{\mathrm{P}}(H_b^v)}{\partial H_b^v}\end{aligned} \tag{2.51}$$

The spring's deformation twist is decomposed by $T_b^{b,v} = T_b^{b,0} - T_v^{b,0}$. The damping along this spring is $W_b^b = D_b T_b^{b,v}$. Body, spring and damper move uniformly with the twist $T_b^{b,0}$ and the wrenches add up. Combing all components we arrive at

$$\begin{pmatrix}\dot{H}_b^0\\ \dot{H}_b^v\\ \dot{P}_b^b\end{pmatrix} = \begin{pmatrix}0 & 0 & H_b^0\\ 0 & 0 & H_b^v\\ -(H_b^0)^T & -(H_b^v)^T & C_b - D_b\end{pmatrix}\begin{pmatrix}\frac{\partial \mathcal{H}}{\partial H_b^0}\\ \frac{\partial \mathcal{H}}{\partial H_b^v}\\ \frac{\partial \mathcal{H}}{\partial P_b^b}\end{pmatrix} + \begin{pmatrix}0 & 0\\ -H_b^v Ad_{H_0^b} & 0\\ D_b Ad_{H_0^b} & I_6\end{pmatrix}\begin{pmatrix}T_v^0\\ W_b^b\end{pmatrix}$$
$$\begin{pmatrix}W_v^{0,0}\\ T_b^{b,0}\end{pmatrix} = \begin{pmatrix}0 & -Ad^T_{H_0^b}(H_b^v)^T & Ad^T_{H_0^b} D_b\\ 0 & 0 & I_6\end{pmatrix}\begin{pmatrix}\frac{\partial \mathcal{H}}{\partial H_b^0}\\ \frac{\partial \mathcal{H}}{\partial H_b^v}\\ \frac{\partial \mathcal{H}}{\partial P_b^b}\end{pmatrix} \tag{2.52}$$

This clearly accounts for an *external* impedance relation, used to establish compliant behaviour between (virtual) object and environment. Analogously we can define impedance relations between manipulators and virtual object. To this purpose we define a manipulator inertia and connect it to the object with a spring and a damper. Here we consider the manipulator masses to be gravity pre-compensated and omit the spring connecting to the ground. The i-th manipulator inertia is given by

$$\begin{aligned} \dot{P}_i^i &= C_i \frac{\partial V_{\mathrm{K}}(P_i^i)}{\partial P_i^i} + I_6 W_i^i \\ T_i^{i,0} &= I_6 \frac{\partial V_{\mathrm{K}}(P_i^i)}{\partial P_i^i} \end{aligned} \tag{2.53}$$

It is important that the spring connecting b and i does not connect to the center of the object b but to a point $b(i)$ on the surface of b. Clearly the distance $p_{b(i)}^b$ corresponds to the extent of the object. The spring's twist decomposes as follows

$$T_{b(i)}^i = T_b^i + T_{b(i)}^{i,b} = Ad_{H_b^i} T_b^{b,0} - T_i^{i,0} + Ad_{H_b^i} \underbrace{T_{b(i)}^b}_{=0} \tag{2.54}$$

The spring is given by

$$\begin{aligned} \dot{H}_{b(i)}^i &= H_{b(i)}^i \begin{pmatrix} Ad_{H_b^{b(i)}} & -Ad_{H_i^{b(i)}} \end{pmatrix} \begin{pmatrix} T_b^{b,0} \\ T_i^{i,0} \end{pmatrix} \\ \begin{pmatrix} W_b^{b,0} \\ W_i^{i,0} \end{pmatrix} &= \begin{pmatrix} Ad^T_{H_b^{b(i)}} \\ -Ad^T_{H_i^{b(i)}} \end{pmatrix} (H_{b(i)}^i)^T \frac{\partial V_{\mathrm{P}}(H_b^{b(i)})}{\partial H_{b(i)}^i} \end{aligned} \tag{2.55}$$

and the damper along the spring exerts a wrench on the body i

$$W_i^i = D_i T_i^{i,b} = D_i T_i^{i,0} - D_i Ad_{H_b^i} T_b^{b,0}. \tag{2.56}$$

We can combine spring, inertia and damper, the twist $T_i^{i,0}$ is the common quantity.

$$\begin{aligned} \begin{pmatrix} \dot{H}_{b(i)}^i \\ \dot{P}_i^i \end{pmatrix} &= \begin{pmatrix} 0 & -H_{b(i)}^i Ad_{H_i^{b(i)}} \\ Ad^T_{H_i^{b(i)}} (H_{b(i)}^i)^T & C_i - D_i \end{pmatrix} \begin{pmatrix} \frac{\partial \mathcal{H}}{\partial H_{b(i)}^i} \\ \frac{\partial \mathcal{H}}{\partial P_i^i} \end{pmatrix} \\ &\quad + \begin{pmatrix} H_{b(i)}^i Ad_{H_b^{b(i)}} & 0 \\ D_i Ad_{H_b^i} & I_6 \end{pmatrix} \begin{pmatrix} T_b^{b,0} \\ W_i^i \end{pmatrix} \\ \begin{pmatrix} W_b^{b,0} \\ T_i^{i,0} \end{pmatrix} &= \begin{pmatrix} Ad^T_{H_b^{b(i)}} (H_{b(i)}^i)^T & Ad^T_{H_b^i} D_i^T \\ 0 & I_6 \end{pmatrix} \begin{pmatrix} \frac{\partial \mathcal{H}}{\partial H_{b(i)}^i} \\ \frac{\partial \mathcal{H}}{\partial P_i^i} \end{pmatrix} \end{aligned} \tag{2.57}$$

2.5 Imposing constraints

The interconnection of a spring and an inertia is the the ideal pair in terms of input-output causality. The spring expects a twist-input and outputs a wrench. The inertia

has a wrench-input and outputs a twist. It can be seen from eq. (2.47) that the interconnection of inertia and spring gives a set of ordinary differential equations (ODEs). Many mechanical systems cannot be modelled by an interconnection of springs and masses. The prime example is the contact of two rigid objects, rigid means there is no elastic deformation which could be modelled by a spring (for an extensive treatment of hard and soft contact see [DS09]). Rigidly connected objects cannot move with respect to each other, i.e. they move uniformly. In cooperative manipulation we often assume the manipulators rigidly connected to the common object. The attempt to move the bodies individually results in *internal* forces. We call a force internal if it produces no *virtual work* with the system's velocity (see [EH16] for a formal definition). The motion-limiting conditions are called kinematic *constraints* and are expressed in the form

$$A^T(\boldsymbol{q})\dot{\boldsymbol{q}} = 0 \tag{2.58}$$

We call $A(\boldsymbol{q}) \in \mathbb{R}^{k\times l}$ the *constraint* matrix, l is the number of independent kinematic constraints. The derivation starts from the Euler-Lagrange equations of constrained motion [DMSB09]

$$\begin{aligned} \frac{d}{dt}\left(\frac{\partial \mathcal{L}}{\dot{\boldsymbol{q}}}\right) - \frac{\partial \mathcal{L}}{\partial \boldsymbol{q}} &= G(\boldsymbol{q})\boldsymbol{u} + A(\boldsymbol{q})\boldsymbol{\lambda} \\ A^T(\boldsymbol{q})\dot{\boldsymbol{q}} &= 0 \end{aligned} \tag{2.59}$$

The associated constraint forces are given by $A(\boldsymbol{q})\boldsymbol{\lambda}$, where we call $\boldsymbol{\lambda} \in \mathbb{R}^l$ the *Lagrange* multipliers. They are uniquely determined if the constraints are satisfied, i.e. are given by the requirement $A^T(\boldsymbol{q})\dot{\boldsymbol{q}} = 0$. In this case the constraint forces do not influence the energy of the system since $\boldsymbol{\lambda}^T(A^T(\boldsymbol{q})\dot{\boldsymbol{q}}) = 0$, this corresponds to the requirement of a zero virtual work for internal forces. Similarly to Section 2.2, the Euler-Lagrange equations can be transformed to a port-Hamiltonian equivalent, which is a mixed set of differential and algebraic equations (DAE).

$$\begin{aligned} \begin{pmatrix} \dot{\boldsymbol{q}} \\ \dot{\boldsymbol{p}} \end{pmatrix} &= \begin{pmatrix} 0 & I \\ -I & 0 \end{pmatrix} \begin{pmatrix} \frac{\partial \mathcal{H}}{\partial \boldsymbol{q}} \\ \frac{\partial \mathcal{H}}{\partial \boldsymbol{p}} \end{pmatrix} + \begin{pmatrix} 0 & 0 \\ A(\boldsymbol{q}) & G(\boldsymbol{q}) \end{pmatrix} \begin{pmatrix} \boldsymbol{\lambda} \\ \boldsymbol{u} \end{pmatrix} \\ \begin{pmatrix} 0 \\ e \end{pmatrix} &= \begin{pmatrix} 0 & A^T(\boldsymbol{q}) \\ 0 & G^T(\boldsymbol{q}) \end{pmatrix} \begin{pmatrix} \frac{\partial \mathcal{H}}{\partial \boldsymbol{p}} \\ \frac{\partial \mathcal{H}}{\partial \boldsymbol{p}} \end{pmatrix} \end{aligned} \tag{2.60}$$

The system is no longer described in the input-state-output form, but in an implicit form. Several approaches to solve the algebraic equations and restore the desired input-state-output form exist. Most of them are designed for generalized configuration $\boldsymbol{q}$ and momentum $\boldsymbol{p}$ coordinates, see e.g. [vdS13],[DS09]. Due to non-linearity of $\dot{\boldsymbol{q}} = \frac{\partial \mathcal{H}}{\partial \boldsymbol{p}}$ in mechanical systems not all are feasible for 3D mechanical systems.
The following method (described e.g. in [DS09]) uses the time-derivative of the constraints

$$0 = \frac{d}{dt}\left(A^T(\boldsymbol{q})\frac{\partial \mathcal{H}}{\partial \boldsymbol{p}}\right) \tag{2.61}$$

We use the property $\frac{\partial \mathcal{H}}{\partial \boldsymbol{p}} = M^{-1}\boldsymbol{p}$ for an energy function of the form $\mathcal{H} = \frac{1}{2}\boldsymbol{p}^T M^{-1}\boldsymbol{p} + V_\mathrm{P}$. Since $\boldsymbol{q}(t)$ is time-variant *indirect dependencies* arise in $A(\boldsymbol{q}), \boldsymbol{p}(\boldsymbol{q})$ when calculating the total time-derivative

$$\begin{aligned} 0 &= \frac{d}{dt}(A^T M^{-1}\boldsymbol{p}) = \frac{\partial (A^T M^{-1}\boldsymbol{p})}{\partial \boldsymbol{q}}\dot{\boldsymbol{q}} + A^T M^{-1}\dot{\boldsymbol{p}} \\ &= \frac{\partial (A^T M^{-1}\boldsymbol{p})}{\partial \boldsymbol{q}} M^{-1}\boldsymbol{p} + A^T M^{-1}\left(-\frac{\partial \mathcal{H}}{\partial \boldsymbol{q}} + A(\boldsymbol{q})\boldsymbol{\lambda} + G(\boldsymbol{q})\boldsymbol{u}\right) \end{aligned} \tag{2.62}$$

Solving this equation for $\boldsymbol{\lambda}$ gives an analytic expression for the constrained forces

$$\boldsymbol{\lambda} = (A^T M^{-1} A)^{-1}\left(-\frac{\partial (A^T M^{-1} p)}{\partial \boldsymbol{q}} M^{-1}\boldsymbol{p} + \frac{\partial \mathcal{H}}{\partial \boldsymbol{q}} - G\boldsymbol{u}\right) \tag{2.63}$$

Then $\boldsymbol{\lambda}$ is re-inserted into eq. (2.60) and we obtain a set of ODEs in input-state-output form. Clearly the term $A(\boldsymbol{q})\boldsymbol{\lambda}$ generates compensation forces, that oppose relative motions of the bodies and keep the constraints $A^T(\boldsymbol{q})\dot{\boldsymbol{q}}$ fulfilled. Since we computed the constraint forces starting from the time-derivative of the constraint, $A^T(\boldsymbol{q})\dot{\boldsymbol{q}}$ stays constant. To guarantee $A^T(\boldsymbol{q})\dot{\boldsymbol{q}} = 0$, this must be already fulfilled in the beginning.

Constraints for 6D-motion

Consider two rigidly connected bodies, associated with the frames Ψ_b and Ψ_i and a distance between them $\boldsymbol{p}_i^b = \boldsymbol{p}_i^0 - \boldsymbol{p}_b^0$. Clearly, in the setting of cooperative manipulation, one can think of an object b and the i-th manipulator attached to it. Now let the body b rotate with the angular velocity $\boldsymbol{\omega}_b^0$. Being rigidly attached the body i rotates in the same manner, $\boldsymbol{\omega}_i^0 = \boldsymbol{\omega}_b^0$. The translational velocity of body i is expressed dependent on body b by

$$\begin{aligned} \dot{\boldsymbol{p}}_i^0 &= \dot{\boldsymbol{p}}_b^0 + \boldsymbol{\omega}_b^0 \times \boldsymbol{p}_i^b = \dot{\boldsymbol{p}}_b^0 + \boldsymbol{\omega}_b^0 \times (\boldsymbol{p}_i^0 - \boldsymbol{p}_b^0) \\ \dot{\boldsymbol{p}}_i^0 - \boldsymbol{\omega}_b^0 \times \boldsymbol{p}_i^0 &= \dot{\boldsymbol{p}}_b^0 - \boldsymbol{\omega}_b^0 \times \boldsymbol{p}_b^0 \end{aligned} \tag{2.64}$$

Recall the definition of the linear velocity component of a twist from eq. (2.27) being $\boldsymbol{v}_i^j = \dot{\boldsymbol{p}}_i^j - \boldsymbol{\omega}_i^j \times \boldsymbol{p}_i^j$. Thus we have $\boldsymbol{v}_i^0 = \boldsymbol{v}_b^0$ and consequently $T_i^0 = T_b^0$. For a system of $i = 1...N$ manipulators we write the constraints

$$0 = A^T T = \begin{pmatrix} -I_3 & 0_3 & I_3 & 0_3 & & & \\ 0_3 & -I_3 & 0_3 & I_3 & & & \\ \vdots & \vdots & & & \ddots & & \\ -I_3 & 0_3 & & & & I_3 & 0_3 \\ 0_3 & -I_3 & & & & 0_3 & I_3 \end{pmatrix} \begin{pmatrix} T_b^0 \\ T_1^0 \\ \vdots \\ T_N^0 \end{pmatrix} \tag{2.65}$$

We start by differentiating the constraints, here A is not time or configuration dependent, thus $0 = A^T \dot{T}$. Consider the simple example of two rigidly connected

bodies b and i, the constraint equation is

$$\begin{aligned} 0 = \dot{T}_i^0 - \dot{T}_b^0 = \begin{pmatrix} \dot{\boldsymbol{\omega}}_i^0 - \dot{\boldsymbol{\omega}}_b^0 \\ \dot{\boldsymbol{v}}_i^0 - \dot{\boldsymbol{v}}_b^0 \end{pmatrix} = \begin{pmatrix} \dot{\boldsymbol{\omega}}_i^0 - \dot{\boldsymbol{\omega}}_b^0 \\ \frac{d}{dt}(\dot{\boldsymbol{p}}_i^0 - \boldsymbol{\omega}_b^0 \times \boldsymbol{p}_i^0) - \frac{d}{dt}(\dot{\boldsymbol{p}}_b^0 - \boldsymbol{\omega}_b^0 \times \boldsymbol{p}_b^0) \end{pmatrix} \\ = \begin{pmatrix} \dot{\boldsymbol{\omega}}_i^0 - \dot{\boldsymbol{\omega}}_b^0 \\ \ddot{\boldsymbol{p}}_i^0 - \ddot{\boldsymbol{p}}_b^0 - \dot{\boldsymbol{\omega}}_b^0 \times \boldsymbol{p}_i^b - \boldsymbol{\omega}_b^0 \times (\boldsymbol{\omega}_b^0 \times \boldsymbol{p}_i^b) \end{pmatrix} \end{aligned} \tag{2.66}$$

Kinematic constraints are expressed very compactly in the twist notation. Second-order dynamics including *centripetal* terms are inherent and equivalent to classic representations (see e.g.[EH16]).

Towards solving the set of port-Hamiltonian DAEs, recall from eq. (2.60) that $0 = A^T \frac{\partial \mathcal{H}}{\partial \boldsymbol{p}}$. At this point it is necessary to distinguish different twist representations, e.g. $\frac{\partial \mathcal{H}}{\partial P_b^b} = T_b^{b,0} = Ad_{H_0^b} T_b^0$. Continuing the two mass example we re-write the constraints

$$0 = A^T \begin{pmatrix} T_b^0 \\ T_i^0 \end{pmatrix} = \underbrace{A^T \begin{pmatrix} Ad_{H_b^0} & 0 \\ 0 & Ad_{H_i^0} \end{pmatrix}}_{\bar{A}^T} \begin{pmatrix} T_b^{b,0} \\ T_i^{i,0} \end{pmatrix} = A^T \begin{pmatrix} Ad_{H_b^0} & 0 \\ 0 & Ad_{H_i^0} \end{pmatrix} \begin{pmatrix} \frac{\partial \mathcal{H}}{\partial P_b^b} \\ \frac{\partial \mathcal{H}}{\partial P_i^i} \end{pmatrix} \tag{2.67}$$

Replacing the twists with momenta $T = M^{-1}P$ and differentiating w.r.t to time leads to

$$0 = \bar{A}^T \begin{pmatrix} M_b^{-1} & 0 \\ 0 & M_i^{-1} \end{pmatrix} \begin{pmatrix} \dot{P}_b^b \\ \dot{P}_i^i \end{pmatrix} + \bar{A}^T \begin{pmatrix} ad_{T_b^{b,0}} & 0 \\ 0 & ad_{T_i^{i,0}} \end{pmatrix} \begin{pmatrix} M_b^{-1} & 0 \\ 0 & M_i^{-1} \end{pmatrix} \begin{pmatrix} P_b^b \\ P_i^i \end{pmatrix} \tag{2.68}$$

Consider now the last part of this equation and recall the adjoint representation ad_T from eq. (2.39). We obtain for body b

$$ad_{T_b^{b,0}} M_b^{-1} P_b^b = \begin{pmatrix} \tilde{\omega}_b^{b,0} & 0 \\ \tilde{v}_b^{b,0} & \tilde{\omega}_b^{b,0} \end{pmatrix} \begin{pmatrix} \boldsymbol{\omega}_b^{b,0} \\ \boldsymbol{v}_b^{b,0} \end{pmatrix} = 0 \tag{2.69}$$

Here we assume that the inertias are not configuration dependent, i.e. time-invariant. Now we insert the port-Hamiltonian system equation for $\dot{P}$ and obtain

$$0 = \bar{A}^T M^{-1} \dot{P} = \bar{A}^T M^{-1}(W + CT + \bar{A}\lambda) \tag{2.70}$$

and solve for λ

$$\lambda = -(\bar{A}^T M^{-1} \bar{A})^{-1} \bar{A}^T M^{-1}(W + CT) \tag{2.71}$$

Consider again the example of two rigidly connected bodies b and i. Let us examine the part $\bar{A}^T M^{-1} CT$ in further detail. Using eq. (2.41) and assuming that the bodies

share the orientation $R_0^b = R_0^i$, we obtain

$$\begin{aligned}\bar{A}^T M^{-1} \begin{pmatrix} C_b T_b^{b,0} \\ C_i T_i^{i,0} \end{pmatrix} &= \bar{A}^T M^{-1} \begin{pmatrix} 0 \\ m_b \tilde{v}_b^{b,0} \boldsymbol{\omega}_b^{b,0} \\ 0 \\ m_i \tilde{v}_i^{i,0} \boldsymbol{\omega}_b^{b,0} \end{pmatrix} = \begin{pmatrix} -I_6 & I_6 \end{pmatrix} \begin{pmatrix} 0 \\ R_b^0 \tilde{v}_b^{b,0} \boldsymbol{\omega}_b^{b,0} \\ 0 \\ R_b^0 \tilde{v}_i^{i,0} \boldsymbol{\omega}_b^{b,0} \end{pmatrix} \\ &= \begin{pmatrix} 0 \\ R_b^0 \tilde{\omega}_b^{b,0} (\tilde{p}_0^b R_b^0 \boldsymbol{\omega}_b^0 + R_0^b \boldsymbol{v}_b^0 - \tilde{p}_0^i R_0^b \boldsymbol{\omega}_b^0 - R_0^b \boldsymbol{v}_i^0) \end{pmatrix} = \begin{pmatrix} 0 \\ R_b^0 \tilde{\omega}_b^{b,0} \tilde{p}_i^b \boldsymbol{\omega}_b^{b,0} \end{pmatrix}\end{aligned} \tag{2.72}$$

This example shows how kinematic constraints can be solved by calculating the constraint forces. The results are equivalent to approaches based on the *Gauss' principle of least constraint* ([EH16]) or *Euler-Lagrange* representations ([LL02]).

2.6 Model-based controllers for cooperative manipulation

In this section we design two model-based control schemes by building virtual structures to achieve a certain group behaviour of the robots. This approach can be viewed in the context of formation control and is also very similar to the *Intrinsically Passive Controller* (IPC) paradigm introduced by Stramigioli [Str01b]. It has the advantages of a physical fundament, passivity and stability during contact and non-contact transitions. Please note that the controller is no more than a geometric interconnection of mechanic elements in a virtual domain.
In formation control the robots are coordinated by connecting them with virtual springs and dampers, the IPC furthermore introduces a virtual object. Our controller design mimics an impedance controlled cooperative manipulation set-up, i.e. the controller has the structure of robots manipulating a common object, see figure 2.3 for an overview.
In this *virtual* set-up the common object and the manipulators are simple inertias. The manipulators connect to the object by springs and dampers, i.e. the connection is compliant. This leads to stability during contact and non-contact transitions.
The scheme is object-centred, i.e. the user controls the object *explicitly* and the controller generates appropriate commands for the robotic system. Explicit here refers to a virtual coupling between the user (i.e. the reference trajectory given by the user) and the virtual object, established by a spring and a damper.
The controller connects the human user and the robot team in form of a shared control approach. Its output to the robots is either a reference trajectory (subsection 2.6.1) or force commands (subsection 2.6.2). The respective dual quantity serves as an input for the controller.
Conclusively the controller is a virtual system model that generates control outputs by simulating the dynamics of its internal structure. Every connection either

between the sub-elements inside the controller or the external ones (user-IPC, IPC-robots) are described by effort-flow pairs, i.e. power ports. From an energetic point of view the interconnection is lossless (see subsection 2.2.1) and the elements are passive, this motivates the term *intrinsic passivity* [Str01b]. By definition a passive controller cannot generate energy, thus energy must be provided from outside, either by the user or by the robotic system, through the power ports.

Stramigioli's original IPC scheme [Str01b] does not incorporate the inertias of the manipulators, nor damping along the manipulator springs, in the controller. For the energy shaping control applied in chapter 3 we require an exact model of the cooperative set-up. The manipulator inertias can be added to the controller in (at least) two ways, leading to the two schemes presented below.

2.6.1 Compliant trajectory generating IPC

Starting from the mechanical impedance equations derived in subsection 2.4, a controller based on the structure of the cooperative manipulation set-up is designed. The starting point is the impedance equation (2.52) accounting for the relation between object and reference trajectory. The inertia M_b represents the common object, spring and damper establish a relation between desired and *actual* object twist. In this context the actual twist is the twist of the simulated object (no object tracking information from the real set-up is used). Analogously to a real cooperative manipulation set-up, the i-manipulators connect to the virtual object. In the controller these connections are compliant (not rigid), i.e. springs are between object and manipulators. The manipulator-object impedance equation (2.57) defines the springs, mass and dampers of the modelled manipulators. One spring hinge-point is connected to the surface of the object, the other hinge point is connected to the impedance relation's inertia M_i, which clearly represents the i-th manipulator's body. In summary a simple geometric interconnection of the impedance equations (2.52,2.57) forms the controller, the structure can be seen from figure 2.4. In place of a full cooperative manipulation set-up with n manipulators we derive the controller for a single manipulator i, the equations for $i = 1...N$ manipulators can be found in the Appendix.

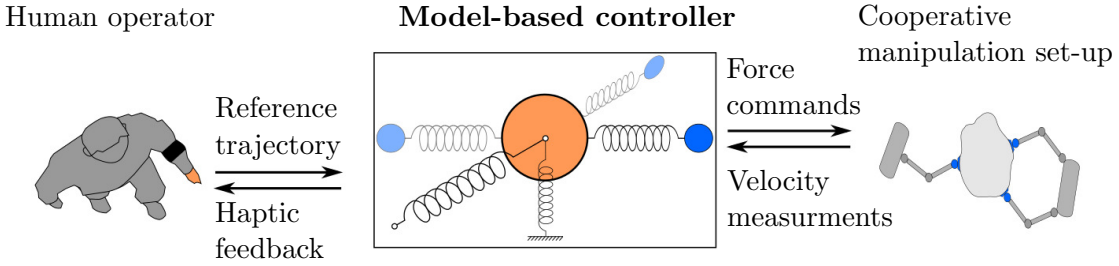

Figure 2.3: Overall set-up

$$\begin{pmatrix} \dot{H}_b^0 \\ \dot{H}_b^v \\ \dot{P}_b^b \\ \dot{H}_{b(i)}^i \\ \dot{P}_i^i \end{pmatrix} = \begin{pmatrix} 0 & 0 & H_b^0 & 0 & 0 \\ 0 & 0 & H_b^v & 0 & 0 \\ -H_b^{0T} & -H_b^{vT} & C_b - D_b & -Ad^T_{H_b^{b(i)}} {H_{b(i)}^i}^T & -Ad^T_{H_b^i} D_i \\ 0 & 0 & H_{b(i)}^i Ad_{H_b^{b(i)}} & 0 & -H_{b(i)}^i Ad_{H_i^{b(i)}} \\ 0 & 0 & D_i Ad_{H_b^i} & Ad^T_{H_i^{b(i)}} {H_{b(i)}^i}^T & C_i - D_i \end{pmatrix} \begin{pmatrix} \frac{\partial \mathcal{H}}{\partial H_b^0} \\ \frac{\partial \mathcal{H}}{\partial H_b^v} \\ \frac{\partial \mathcal{H}}{\partial P_b^b} \\ \frac{\partial \mathcal{H}}{\partial H_{b(i)}^i} \\ \frac{\partial \mathcal{H}}{\partial P_i^i} \end{pmatrix} + \begin{pmatrix} 0 & 0 \\ -H_b^v Ad_{H_0^b} & 0 \\ D_b Ad_{H_0^b} & 0 \\ 0 & 0 \\ 0 & I_6 \end{pmatrix} \begin{pmatrix} T_v^0 \\ W_i^i \end{pmatrix} \tag{2.73}$$

$$\begin{pmatrix} W_v^{0,0} \\ T_i^{i,0} \end{pmatrix} = \begin{pmatrix} 0 & -Ad^T_{H_0^b} H_b^{vT} & Ad^T_{H_0^b} D_b^T & 0 & 0 \\ 0 & 0 & 0 & 0 & I_6 \end{pmatrix} \begin{pmatrix} \frac{\partial \mathcal{H}}{\partial H_b^0} \\ \frac{\partial \mathcal{H}}{\partial H_b^v} \\ \frac{\partial \mathcal{H}}{\partial P_b^b} \\ \frac{\partial \mathcal{H}}{\partial H_{b(i)}^i} \\ \frac{\partial \mathcal{H}}{\partial P_i^i} \end{pmatrix}$$

Note that the output to the robot side is a twist, the control scheme thus generates a compliant reference trajectory for the robots to follow. Similar to [CCMV08] we require a local underlying force control layer to operate the robots.

Passivity

Passivity follows directly from the port-Hamiltonian formulation, the above representation is of the standard from (2.10). The terms to be omitted due to the skew-symmetry of the structure matrix $J(x)$ are not given in the following energy

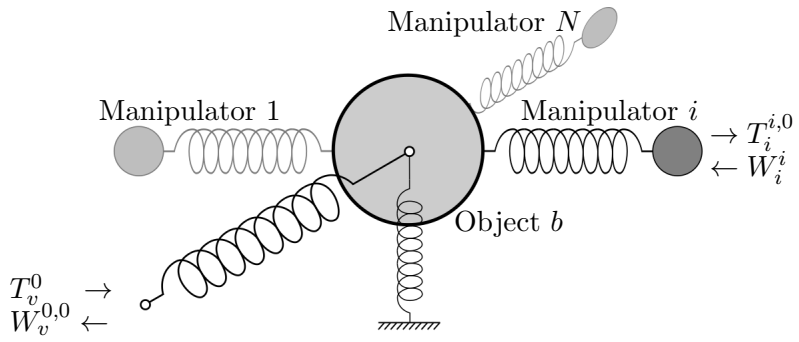

Figure 2.4: Compliant reference trajectory generating controller

balance

$$\begin{aligned}\dot{\mathcal{H}} &= -\frac{\partial^T \mathcal{H}}{\partial P_b^b} D_b \frac{\partial \mathcal{H}}{\partial P_b^b} - \frac{\partial^T \mathcal{H}}{\partial P_i^i} D_i \frac{\partial \mathcal{H}}{\partial P_i^i} \\ &- \frac{\partial^T \mathcal{H}}{\partial H_b^v} H_b^v Ad_{H_0^b} T_v^0 + \frac{\partial^T \mathcal{H}}{\partial P_b^b} D_b Ad_{H_0^b} T_v^0 + \frac{\partial^T \mathcal{H}}{\partial P_i^i} W_i^i \\ &= \underbrace{-\frac{\partial^T \mathcal{H}}{\partial P_b^b} D_b \frac{\partial \mathcal{H}}{\partial P_b^b} - \frac{\partial^T \mathcal{H}}{\partial P_i^i} D_i \frac{\partial \mathcal{H}}{\partial P_i^i}}_{\text{dissipation}} + \underbrace{W_v^{0,0^T} T_v^0 + T_i^{i,0^T} W_i^i}_{\text{inputs}}\end{aligned} \tag{2.74}$$

I.e. the controller is passive, this is a sufficient condition for asymptotic stability.

2.6.2 Constrained dynamics IPC

In a robotic set-up velocities are easier to measure than forces. From this point of view it is convenient to design a controller that issues force commands to the robots and receives velocity feedback. The difficulty to overcome here is the *preferred causality* of port-Hamiltonian elements. Please note from subsection 2.3.3 that springs expect a twist for input and output a wrench. Vice versa inertias accept a wrench input, resulting in a twist output. In this formulations the state variable is computed by integration over time, opposite causality representations are possible but require the time derivative. Numerical differentiation amplifies numerical noise, thus the integration form is the preferred one. Furthermore integration allows to use information in form of initial conditions, while differentiation does not. For more information on causality see [DMSB09].
In the controller both the virtual object and the robotic system expect wrenches, in terms of causality calling for a spring. Therefore a virtual manipulator inertia is added by rigidly connecting it to the virtual object, figure 2.5 illustrates the composition. In a real cooperative manipulation set-up it is also common to have this rigid connection between end-effector and object, making this an obvious choice for control.
Rigid coupling of a manipulator and the object is treated with the approach presented in section 2.5. Once again we start from a single manipulator i in place of a full cooperative manipulation set-up. Bodies b and $b(i)$ are rigidly connected and their port-Hamiltonian equations are

$$\begin{aligned}\begin{pmatrix} \dot{P}_b^b \\ \dot{P}_{b(i)}^{b(i)} \end{pmatrix} &= \begin{pmatrix} C_b & 0 \\ 0 & C_{b(i)} \end{pmatrix} \begin{pmatrix} \frac{\partial \mathcal{H}}{\partial P_b^b} \\ \frac{\partial \mathcal{H}}{\partial P_{b(i)}^{b(i)}} \end{pmatrix} + \begin{pmatrix} W_b^b \\ W_{b(i)}^{b(i)} \end{pmatrix} + \bar{A}\boldsymbol{\lambda} \\ 0 &= \bar{A}^T \begin{pmatrix} \frac{\partial V}{\partial P_b^b} \\ \frac{\partial V}{\partial P_{b(i)}^{b(i)}} \end{pmatrix}\end{aligned} \tag{2.75}$$

The Lagrange multipliers are eliminated as shown in section 2.5. In order to write

the full control scheme in a compact notation we introduce four abbreviations accounting for the constrained forces

$$\begin{aligned}
\mathcal{A}_b^b &= Ad_{H_b^0}^T (\bar{A}^T M^{-1} \bar{A})^{-1} Ad_{H_b^0} M_b^{-1} \\
\mathcal{A}_b^i &= Ad_{H_b^0}^T (\bar{A}^T M^{-1} \bar{A})^{-1} Ad_{H_{b(i)}^0} M_{b(i)}^{-1} \\
\mathcal{A}_i^b &= Ad_{H_{b(i)}^0}^T (\bar{A}^T M^{-1} \bar{A})^{-1} Ad_{H_b^0} M_b^{-1} \\
\mathcal{A}_i^i &= Ad_{H_{b(i)}^0}^T (\bar{A}^T M^{-1} \bar{A})^{-1} Ad_{H_{b(i)}^0} M_{b(i)}^{-1}
\end{aligned} \tag{2.76}$$

$$\begin{aligned}
\begin{pmatrix} \dot{H}_b^0 \\ \dot{H}_b^v \\ \dot{P}_b^b \\ \dot{H}_{b(i)}^i \\ \dot{P}_{b(i)}^{b(i)} \end{pmatrix} &= \begin{pmatrix} 0 & 0 & H_b^0 & 0 & 0 \\ 0 & 0 & H_b^v & 0 & 0 \\ (\mathcal{A}_b^b - I) H_b^{0T} & (\mathcal{A}_b^b - I) H_b^{vT} & (I - \mathcal{A}_b^b)(C_b - D_b) & -\mathcal{A}_b^i {H_{b(i)}^i}^T & \mathcal{A}_b^i (C_{b(i)} - D_{b(i)}) \\ 0 & 0 & 0 & 0 & H_{b(i)}^i \\ -\mathcal{A}_i^b H_b^{0T} & -\mathcal{A}_i^b H_b^{vT} & \mathcal{A}_i^b (C_b - D_b) & (\mathcal{A}_i^i - I) {H_{b(i)}^i}^T & (I - \mathcal{A}_i^i)(C_{b(i)} - D_{b(i)}) \end{pmatrix} \begin{pmatrix} \frac{\partial V}{\partial H_b^0} \\ \frac{\partial V}{\partial H_b^v} \\ \frac{\partial V}{\partial P_b^b} \\ \frac{\partial V}{\partial H_{b(i)}^i} \\ \frac{\partial V}{\partial P_{b(i)}^{b(i)}} \end{pmatrix} \\
&+ \begin{pmatrix} 0 & 0 \\ -H_b^v Ad_{H_0^b} & 0 \\ (I - \mathcal{A}_b^b) D_b Ad_{H_0^b} & \mathcal{A}_b^i D_{b(i)} Ad_{H_0^{b(i)}} \\ 0 & -H_{b(i)}^i Ad_{H_0^{b(i)}} \\ \mathcal{A}_i^b D_b Ad_{H_0^b} & (I - \mathcal{A}_i^i) D_{b(i)} Ad_{H_0^{b(i)}} \end{pmatrix} \begin{pmatrix} T_v^0 \\ T_i^0 \end{pmatrix}
\end{aligned} \tag{2.77}$$

$$\begin{pmatrix} W_v^{0,0} \\ W_i^{0,0} \end{pmatrix} = \begin{pmatrix} 0 & -Ad_{H_0^b}^T H_b^{vT} & Ad_{H_0^b}^T D_b^T (I - \mathcal{A}_b^{bT}) & 0 & Ad_{H_0^b}^T D_b^T \mathcal{A}_i^{bT} \\ 0 & 0 & Ad_{H_0^{b(i)}}^T D_{b(i)}^T \mathcal{A}_b^{iT} & -Ad_{H_0^{b(i)}}^T {H_{b(i)}^i}^T & Ad_{H_0^{b(i)}}^T D_{b(i)}^T (I - \mathcal{A}_i^{iT}) \end{pmatrix} \begin{pmatrix} \frac{\partial V}{\partial H_b^0} \\ \frac{\partial V}{\partial H_b^v} \\ \frac{\partial V}{\partial P_b^b} \\ \frac{\partial V}{\partial H_{b(i)}^i} \\ \frac{\partial V}{\partial P_{b(i)}^{b(i)}} \end{pmatrix}$$

Passivity

Unlike to the previous, a number of elements with no skew-symmetric counterpart is apparent in the structure matrix. However the property of lossless interconnection

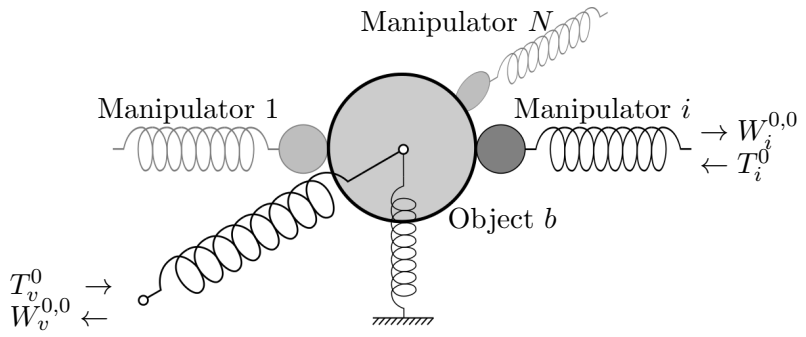

Figure 2.5: Structure of the constrained dynamic IPC

still holds, omitting the skew-symmetric elements we have

$$\dot{V} = \begin{pmatrix} \frac{\partial \mathcal{H}}{\partial P_b^b} \\ \frac{\partial \mathcal{H}}{\partial P_{b(i)}^{b(i)}} \end{pmatrix}^T \begin{pmatrix} \mathcal{A}_b^b H_b^{0T} & \mathcal{A}_b^b H_b^{vT} & -\mathcal{A}_b^b (C_b - D_b) & -\mathcal{A}_b^i H_{b(i)}^{i\ T} & \mathcal{A}_b^i (C_{b(i)} - D_{b(i)}) \\ -\mathcal{A}_i^b H_b^{0T} & -\mathcal{A}_i^b H_b^{vT} & \mathcal{A}_i^b (C_b - D_b) & \mathcal{A}_i^i H_{b(i)}^{i\ T} & -\mathcal{A}_i^i (C_{b(i)} - D_{b(i)}) \end{pmatrix} \begin{pmatrix} \frac{\partial \mathcal{H}}{\partial H_b^0} \\ \frac{\partial \mathcal{H}}{\partial H_b^v} \\ \frac{\partial \mathcal{H}}{\partial P_b^b} \\ \frac{\partial \mathcal{H}}{\partial H_{b(i)}^i} \\ \frac{\partial \mathcal{H}}{\partial P_{b(i)}^{b(i)}} \end{pmatrix} \tag{2.78}$$
$$- \frac{\partial^T \mathcal{H}}{\partial P_b^b} D_b \frac{\partial \mathcal{H}}{\partial P_b^b} - \frac{\partial^T \mathcal{H}}{\partial P_{b(i)}^{b(i)}} D_{b(i)} \frac{\partial \mathcal{H}}{\partial P_{b(i)}^{b(i)}} + W_v^{0,0^T} T_v^0 + W_i^{0,0^T} T_i^0$$

The bodies b and $b(i)$ are rigidly connected, i.e. their twists are related by $T_b^0 = Ad_{H_b^0} T_b^{b,0} = Ad_{H_{b(i)}^0} T_{b(i)}^{b(i),0} = T_{b(i)}^0$. In the upper equation the twists are given by $T_b^{b,0} = \frac{\partial \mathcal{H}}{\partial P_b^b}$ and $T_{b(i)}^{b(i),0} = \frac{\partial \mathcal{H}}{\partial P_{b(i)}^{b(i)}}$. Multiplying with the constraint force terms leads to

$$\begin{aligned} \frac{\partial^T \mathcal{H}}{\partial P_{b(i)}^{b(i)}} \mathcal{A}_i^b &= \frac{\partial^T \mathcal{H}}{\partial P_b^b} Ad_{H_b^{b(i)}}^T \mathcal{A}_i^b = \frac{\partial^T \mathcal{H}}{\partial P_b^b} (Ad_{H_{b(i)}^0} Ad_{H_b^{b(i)}})^T (\bar{A}^T M^{-1} \bar{A})^{-1} Ad_{H_b^0} M_b^{-1} \\ &= \frac{\partial^T \mathcal{H}}{\partial P_b^b} Ad_{H_b^0}^T (\bar{A}^T M^{-1} \bar{A})^{-1} Ad_{H_b^0} M_b^{-1} = \frac{\partial^T \mathcal{H}}{\partial P_b^b} \mathcal{A}_b^b \end{aligned} \tag{2.79}$$

and

$$\begin{aligned} \frac{\partial^T \mathcal{H}}{\partial P_{b(i)}^{b(i)}} \mathcal{A}_i^i &= \frac{\partial^T \mathcal{H}}{\partial P_b^b} Ad_{H_b^{b(i)}}^T \mathcal{A}_i^i = \frac{\partial^T \mathcal{H}}{\partial P_b^b} (Ad_{H_{b(i)}^0} Ad_{H_b^{b(i)}})^T (\bar{A}^T M^{-1} \bar{A})^{-1} Ad_{H_{b(i)}^0} M_b^{-1} \\ &= \frac{\partial^T \mathcal{H}}{\partial P_b^b} Ad_{H_b^0}^T (\bar{A}^T M^{-1} \bar{A})^{-1} Ad_{H_{b(i)}^0} M_b^{-1} = \frac{\partial^T \mathcal{H}}{\partial P_b^b} \mathcal{A}_b^i. \end{aligned} \tag{2.80}$$

The energy balance reduces to the dissipative terms and input-output pairs, the controller is thus passive.

$$\dot{\mathcal{H}} = - \frac{\partial^T \mathcal{H}}{\partial P_b^b} D_b \frac{\partial \mathcal{H}}{\partial P_b^b} - \frac{\partial^T \mathcal{H}}{\partial P_{b(i)}^{b(i)}} D_{b(i)} \frac{\partial V}{\partial P_{b(i)}^{b(i)}} + W_v^{0,0^T} T_v^0 + W_i^{0,0^T} T_i^0 \tag{2.81}$$

Chapter 3

Energy regulating control

Towards a conclusion on stability of the overall system, it is necessary to take the environmental conditions into consideration. Letting a human explicitly control a cooperative robot-team rises the question of her/his dynamic behaviour and the impact on the system. Furthermore the environment, the robotic system is interacting with, can change unexpectedly. Thus stability considerations based on certain environment models may lose their basis. Preserving stability is especially crucial when the human operator is on-site to ensure her/his safety. The objective of this chapter is to introduce an energy tank along with a suitable re-filling strategy, that sources the controller. This maintains a safe level of energy in the system, regardless of the dynamics of a human and the environment. The energy-based controllers from section 2.6 integrate seamlessly with the tank concept.

3.1 Passivity and safe energy levels

Passivity is a key concept when dealing with unknown environments. It is well known that passive robotic systems are stable with any environment, regardless its structure or complexity, that can provide only a bounded amount of energy. On the other hand it is shown in [Str15], that for a non-passive robotic system, there always exists a (passive) environment that destabilizes the overall behaviour.
When a human operator controls a robotic set-up by hand motion, it is often argued that the human arm is not distinguishable from a mechanical impedance. This stems from experiments with a human manipulating a controlled impedance [Hog89]. The robotic device applies a force to the human and s/he responds with motion, therefore the human-machine interface is on an energetic level (the product of force and velocity is mechanical power). In recent years new input methods appeared (hand tracking, gesture control). Here the interaction between human and robotic system is an exchange of information. There is no explicit relation between force and velocity (impedance) and therefore it is not meaningful to model the human operator with an impedance. Feedback given through tactile or visual information does not effectively restrict the operator's motion, allowing him to issue nearly

arbitrary commands. Please recall the introductory example of a robotic system driven into an obstacle. If the user persists to command motion in the blocked direction, then s/he can supply an infinite amount of energy to the system. Figure 3.1 illustrates the exchange of energy of a passive robotic team with the environment and an operator, who directly powers the controller.
In order to obtain a safe and stable human-guided robotic system we propose to assign the operator with an energy budget at disposal to issue commands. The structure is shown in figure 3.2 and the theory treated in the next section. This allows to achieve stability with any environment the robotic system is interacting with, as long as its energy supply is bounded. Using the concept of passivity, asymptotic stability is given without requiring certain models or assumptions for the human and the environment.
For physical human-robot interaction various safety metrics exist, see [Had14] for an overview. We limit our focus to energy-based injury criteria. Experimental studies indicate minimal amounts of energy that cause cranial bone failure [Woo71] or fracture of neck bones [YPM+96]. The results provide a maximum amount of energy to be stored in the cooperative set-up

$$V_{\mathrm{K,Limit}} = \begin{cases} 517\ \mathrm{J} & \text{adult cranium bone failure} \\ 127\ \mathrm{J} & \text{infant cranium bone failure} \\ 30\ \mathrm{J} & \text{neck fracture} \end{cases} \tag{3.1}$$

The model-based controllers designed in section 2.6 simulate the energetic state of the full cooperative set-up. The Hamiltonian energy function of the controller directly resembles the energy level of the real system. The control behaviour is adapted to shape the energetic state both in the controller and in the controlled set-up to maintain a safe state.

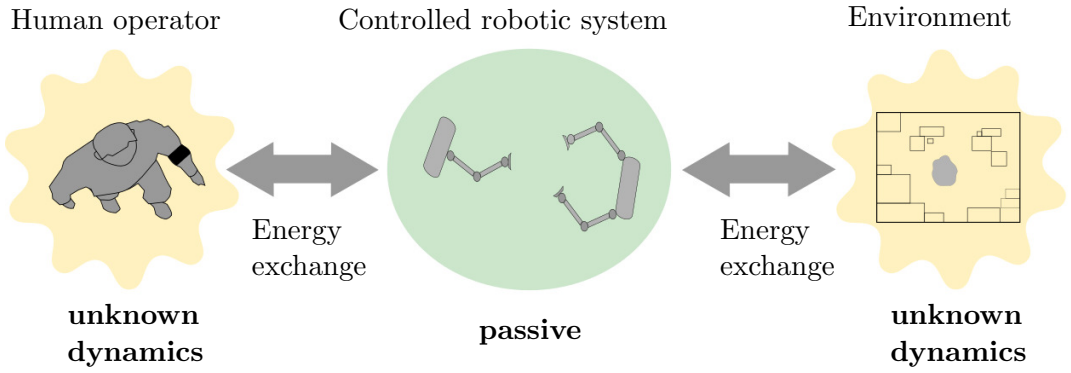

Figure 3.1: The robotic system interacting with operator and environment

3.2 Energy tanks

The motivation for the use of an *energy tank* is to energetically decouple the human operator from the robotic system, i.e. the operator is no longer able to supply energy to the system. This is a consequence of the chosen input method, which is based on information rather than on energy exchange, as discussed above. The energy necessary for driving the robotic system comes from the tank, the operator only controls the energetic flow.
On command of the operator energy flows from the energy tank into the controller and on into the robotic system. Under ideal conditions energy is circulating between these parts and the total amount stays constant (lossless system). In subsection 3.2.2 we discuss cases of a permanent change of the energy balance. At first we examine the combination of an energy tank and a controller as defined in section 2.6. Therefore we assume that no energy is exchanged with the robotic system. In this case we can guarantee a lossless combined system by re-harvesting the energy dissipated in the controller's dampers.
The energy tank is a virtual storage element defined with a Hamiltonian energy function. Let $x_\mathrm{t} \in \mathbb{R}$ denote the (scalar) energy state and we have a simple, positive definite function $\mathcal{T}(x_\mathrm{t}) = \frac{1}{2}x_\mathrm{t}^2$. The dynamic equations of the tank are

$$\begin{aligned} \dot{x_\mathrm{t}} &= f_\mathrm{t} \\ e_\mathrm{t} &= \frac{\partial \mathcal{T}(x_\mathrm{t})}{\partial x_\mathrm{t}} (= x_\mathrm{t}) \end{aligned} \tag{3.2}$$

Here $(f_\mathrm{t}, e_\mathrm{t})$ is the flow-effort pair, corresponding to input and output respectively. Towards the application of the energy tank we consider an example port-Hamiltonian system of the form

$$\begin{aligned} \dot{\boldsymbol{x}} &= [J(\boldsymbol{x}) - R(\boldsymbol{x})]\frac{\partial \mathcal{H}}{\partial \boldsymbol{x}} + G(\boldsymbol{x})\boldsymbol{u} \\ \boldsymbol{y} &= G^T(\boldsymbol{x})\frac{\partial \mathcal{H}}{\partial \boldsymbol{x}} \end{aligned} \tag{3.3}$$

This standard system is chosen to keep the derivation process simple and can be replaced with the controllers from section 2.6. First we seek to re-route the dissipated energy into the energy tank, this is accomplished by choosing the tank input as $f_\mathrm{t} = \frac{1}{x_\mathrm{t}}\frac{\partial^T \mathcal{H}}{\partial \boldsymbol{x}} R(\boldsymbol{x}) \frac{\partial \mathcal{H}}{\partial \boldsymbol{x}} + \tilde{f}_\mathrm{t}$. With a new input $\tilde{f}_\mathrm{t}$ we have the tank's energy balance

$$\dot{\mathcal{T}}(x_\mathrm{t}) = e_\mathrm{t} f_\mathrm{t} = \frac{\partial^T \mathcal{H}}{\partial \boldsymbol{x}} R(\boldsymbol{x}) \frac{\partial \mathcal{H}}{\partial \boldsymbol{x}} + x_\mathrm{t}\tilde{f}_\mathrm{t} \tag{3.4}$$

This corresponds to the systems dissipated energy plus some external supply. Next we use this external supply to interconnect tank and port-Hamiltonian system. A power-preserving interconnection is established, here we use a combination of gyrator and transformer with ratio n

$$\begin{aligned} \boldsymbol{u} &= \boldsymbol{n} e_\mathrm{t} \\ \tilde{f}_\mathrm{t} &= -\boldsymbol{n}^T \boldsymbol{y} \end{aligned} \tag{3.5}$$

By construction and independent of a particular choice of $\boldsymbol{n}$ this relation is power-continuous

$$\boldsymbol{u}^T\boldsymbol{y} = e_{\mathrm{t}}^T\boldsymbol{n}^T\boldsymbol{y} = -e_{\mathrm{t}}^T\tilde{f}_{\mathrm{t}} \tag{3.6}$$

The combined Hamiltonian energy function of the interconnected system is $\bar{\mathcal{H}}(\boldsymbol{x}, x_{\mathrm{t}}) = \mathcal{H}(\boldsymbol{x})+\mathcal{T}(x_{\mathrm{t}})$. The choice of $\boldsymbol{n}$ is not fixed but can be adjusted dynamically to shape the energy flow. In particular it is appealing to use $\boldsymbol{n}$ to replicate the original control signal by choosing $\boldsymbol{n} = \frac{\boldsymbol{w}}{x_{\mathrm{t}}}$. The new control input $\boldsymbol{w}$ can effectively take the role of $\boldsymbol{u}$, i.e. the port-Hamiltonian system becomes

$$\dot{\boldsymbol{x}} = [J(\boldsymbol{x}) - R(\boldsymbol{x})]\frac{\partial\bar{\mathcal{H}}}{\partial\boldsymbol{x}} + G(\boldsymbol{x})\frac{\boldsymbol{w}}{x_{\mathrm{t}}}e_{\mathrm{t}} = [J(\boldsymbol{x}) - R(\boldsymbol{x})]\frac{\partial\bar{\mathcal{H}}}{\partial\boldsymbol{x}} + G(\boldsymbol{x})\boldsymbol{w} \tag{3.7}$$

For a $x_{\mathrm{t}} \to 0$, i.e. an empty energy tank, there is a singularity. Thus an complete depletion of the tank must be avoided. A minimum strategy is to introduce a switching parameter α, we set $\boldsymbol{n} = \frac{\alpha\boldsymbol{w}}{x_{\mathrm{t}}}$ with

$$\alpha = \begin{cases} 1 & \text{if } \mathcal{T}(x_{\mathrm{t}}) \geq \epsilon > 0 \\ 0 & \text{if } \mathcal{T}(x_{\mathrm{t}}) < \epsilon \end{cases} \tag{3.8}$$

This means that a control input is executed unchanged as long as certain amount ϵ of energy is in the tank. Once the energy budget is exceeded and command execution possibly violates passivity the input is set to 0, effectively suspending energy exchange. This happens in both ways, neither is it possibly to re-transfer into the tank through the interconnection. At this point the tank can only be refilled by dissipation. Dissipation is associated with kinetic energy, as long as the system is moving it can recover from the input-suspended state. If the system is driven to a state of exclusively potential energy, there is no dissipation and a deadlock is reached.

Reaching a state of exclusively potential energy takes infinite time, this is because a state of higher potential energy can only be reached by motion. I.e. kinetic energy is a predecessor of potential energy. A fragment of the kinetic energy is dissipated and is available in the energy budget again. The available energy approaches ϵ asymptotically.

Another apparent issue with the binary parameter α is the abrupt switching behaviour if the tank level is in the neighbourhood of ϵ. Numeric simulations indicate high forces and chattering behaviour.

A solution to this desired behaviour is to make α a function of the tank level and continuously scale the desired trajectory.

$$\alpha = \begin{cases} 1 & \text{if } \mathcal{T}(x_{\mathrm{t}}) \geq \mathcal{T}_{th} \\ \frac{T(x_{\mathrm{t}})-\epsilon}{\mathcal{T}_{\mathrm{th}}} & \text{if } \epsilon \leq \mathcal{T}(x_{\mathrm{t}}) < \mathcal{T}_{\mathrm{th}} \\ 0 & \mathcal{T}(x_{\mathrm{t}}) < \epsilon \end{cases} \tag{3.9}$$

Here $\mathcal{T}_{\mathrm{th}} > \epsilon$ is a threshold level that defines the width of the transition region. Adapting the reference trajectory leads to a permanent position deviation, if the

user does not actively readjust after the tank level has recovered. We approach this problem in the next subsection.
Regardless of a particular choice of α we can give a combined port-Hamiltonian representation of the system and the tank

$$\begin{pmatrix} \dot{\boldsymbol{x}} \\ \dot{x}_\mathrm{t} \end{pmatrix} = \left[\begin{pmatrix} J(\boldsymbol{x}) & \frac{\alpha \boldsymbol{w}}{x_\mathrm{t}} \\ -\frac{\alpha \boldsymbol{w}^T}{x_\mathrm{t}} & 0 \end{pmatrix} - \begin{pmatrix} R(\boldsymbol{x}) & 0 \\ -\frac{1}{x_\mathrm{t}} \frac{\partial^T \bar{\mathcal{H}}}{\partial \boldsymbol{x}} R(\boldsymbol{x}) & 0 \end{pmatrix} \right] \begin{pmatrix} \frac{\partial \bar{\mathcal{H}}}{\partial \boldsymbol{x}} \\ \frac{\partial \bar{\mathcal{H}}}{\partial x_\mathrm{t}} \end{pmatrix} \tag{3.10}$$

Note that there is no more an input-output port, this is because ports are defined by energy exchange of the system with its environment. It is shown in subsection 2.2.1 that the systems consistent with (2.10) are passive, analogously we show that the described combination of such a system and the energy tank is *lossless*.

$$\begin{aligned} \frac{d}{dt} \bar{\mathcal{H}}(\boldsymbol{x}, x_\mathrm{t}) &= \begin{pmatrix} \frac{\partial^T \bar{\mathcal{H}}}{\partial \boldsymbol{x}} & \frac{\partial^T \bar{\mathcal{H}}}{\partial x_\mathrm{t}} \end{pmatrix} \begin{pmatrix} \dot{\boldsymbol{x}} \\ \dot{x}_\mathrm{t} \end{pmatrix} = \frac{\partial^T \bar{\mathcal{H}}}{\partial \boldsymbol{x}} J(\boldsymbol{x}) \frac{\partial \bar{\mathcal{H}}}{\partial \boldsymbol{x}} + \frac{\partial^T \bar{\mathcal{H}}}{\partial \boldsymbol{x}} \frac{\alpha \boldsymbol{w}}{x_\mathrm{t}} \frac{\partial \bar{\mathcal{H}}}{\partial x_\mathrm{t}} \\ &- \frac{\partial^T \bar{\mathcal{H}}}{\partial \boldsymbol{x}} R(\boldsymbol{x}) \frac{\partial \bar{\mathcal{H}}}{\partial \boldsymbol{x}} - \frac{\partial^T \bar{\mathcal{H}}}{\partial x_\mathrm{t}} \frac{\alpha \boldsymbol{w}^T}{x_\mathrm{t}} \frac{\partial \bar{\mathcal{H}}}{\partial \boldsymbol{x}} + \frac{\partial^T \bar{\mathcal{H}}}{\partial x_\mathrm{t}} \frac{1}{x_\mathrm{t}} \frac{\partial^T \bar{\mathcal{H}}}{\partial \boldsymbol{x}} R(\boldsymbol{x}) \frac{\partial \bar{\mathcal{H}}}{\partial \boldsymbol{x}} = 0 \end{aligned} \tag{3.11}$$

3.2.1 Energy-adapted stiffness and damping

With the above conjunction of tank and controller control inputs are discarded, as soon as the energy tank is depleted. It is clear that desired trajectories driving the tank to a negative state are not feasible with the given energy budget and need to be altered. Simply discarding the desired trajectory information leads to a permanent deviation of the position. Thus we demand a controller that returns onto the desired trajectory as soon as the energy level has recovered.
Therefore we propose the use of an energy-adapted spring and damper. The idea is to relax the stiffness of the user-object spring as function of the available energy. Actually the impedance of the human hand behaves similar, usually it is stiff for

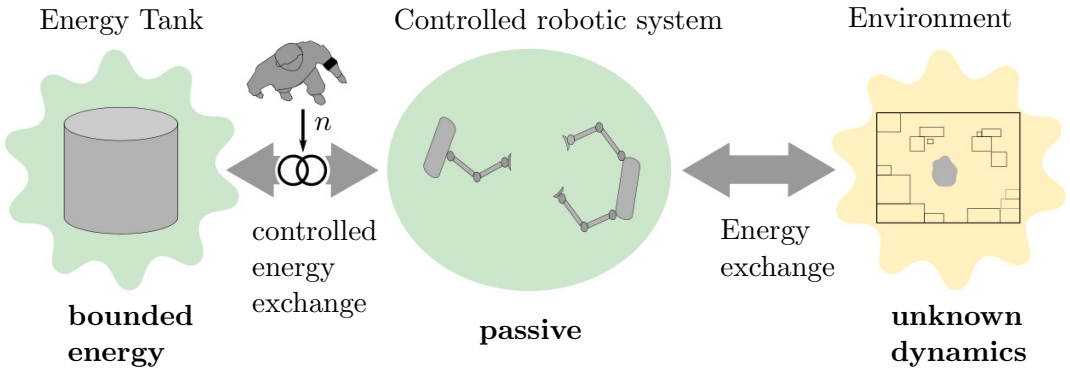

Figure 3.2: The human operator controls the energy flow between tank and robotic system

slow motion and compliant during fast movements (high kinetic energy, likely depleted energy tank) [Hog84a]. A lower stiffness allows the system to "float" loosely, while the tank gets re-filled through the damping.
Moreover a change of stiffness affects the energy stored in the spring, relaxing stiffness sets energy free, which is re-fed into the tank. With a rise of the tank level, stiffness is increased and the spring re-directs the system onto the desired trajectory. To illustrate the principle we start with an example one-dimensional spring given by

$$F = k_{vb}(x_v - x_b)\ ,\ \mathcal{T}(x_\mathrm{t}) \geq \mathcal{T}_\mathrm{th} \tag{3.12}$$

This equation is valid if the tank level $\mathcal{T}(x_\mathrm{t})$ is above a certain threshold level $\mathcal{T}_\mathrm{th}$. The spring's stiffness $k_{vb} \in \mathbb{R}^+$ is unaltered, $x_v, x_b \in \mathbb{R}$ denote the reference and the actual position respectively. Below the threshold we propose the following spring function

$$F = k_{vb}\frac{\mathcal{T}(x_\mathrm{t})}{\mathcal{T}_\mathrm{th}}(x_v - x_b)\ ,\ \mathcal{T}(x_\mathrm{t}) < \mathcal{T}_\mathrm{th} \tag{3.13}$$

For ease of notation we define a new stiffness parameter

$$\kappa = \begin{cases} k_{vb} & \text{if } \mathcal{T}(x_\mathrm{t}) \geq \mathcal{T}_\mathrm{th} \\ k_{vb}\frac{\mathcal{T}(x_\mathrm{t})}{\mathcal{T}_\mathrm{th}} & \text{if } \mathcal{T}(x_\mathrm{t}) < \mathcal{T}_\mathrm{th} \end{cases} \tag{3.14}$$

The corresponding energy function is then

$$V_\kappa(x_v, x_b, \kappa) = \frac{1}{2}\kappa(x_v - x_b)^2 \tag{3.15}$$

The exchanged power with respect to a change of stiffness is

$$\dot{V}_\kappa = \frac{\partial V_\kappa}{\partial \kappa}\frac{d\kappa}{dt} = \frac{1}{2}(x_v - x_b)^2\dot{\kappa} = e_\mathrm{k}^T f_\mathrm{k}, \tag{3.16}$$

which corresponds to the product of effort ($\frac{\partial V_\kappa}{\partial \kappa}$) and flow ($\dot{\kappa}$) and forms a power port ($f_\mathrm{k}, e_\mathrm{k}$) as defined in Section 2.2. The energy function of a 6-DoF spring is of the from

$$V_\kappa : SE(3) \times \mathcal{K} \to \mathbb{R}; (H_b^v, \kappa) \mapsto V_\kappa(H_b^v, \kappa), \tag{3.17}$$

which is equal to the previous spring energy function (eq. (2.35)) but depends explicitly on the stiffness parameter κ. $\mathcal{K}$ is a parametric space that equals $\mathbb{R}$ in case of an isotropic spring. For more information on variable spatial springs see [SD01]. The port-Hamiltonian representation of a variable stiffness spring is given by

$$\begin{aligned} \begin{pmatrix} \dot{H}_b^v \\ \dot{\kappa} \end{pmatrix} &= \begin{pmatrix} H_b^v & 0 \\ 0 & I \end{pmatrix} \begin{pmatrix} T_b^{b,v} \\ f_\mathrm{k} \end{pmatrix} \\ \begin{pmatrix} W_b^{b,v} \\ e_\mathrm{k} \end{pmatrix} &= \begin{pmatrix} H_b^{vT} & 0 \\ 0 & I \end{pmatrix} \begin{pmatrix} \frac{\partial V_\kappa}{\partial H_b^v} \\ \frac{\partial V_\kappa}{\partial \kappa} \end{pmatrix}, \end{aligned} \tag{3.18}$$

where $f_\mathrm{k}, e_\mathrm{k}$ is the input-output pair. Towards pairing the variable stiffness spring with the energy tank we can express κ as a function of the tank level. By using the tank power flow equation (3.4) we obtain

$$\dot{\kappa} = \begin{cases} 0 & \text{if } \mathcal{T}(x_\mathrm{t}) \geq \mathcal{T}_\mathrm{th} \\ \frac{k}{\mathcal{T}_\mathrm{th}} \dot{\mathcal{T}}(x_\mathrm{t}) = \frac{k_{vb}}{T_\mathrm{th}} \dot{x}_\mathrm{t} \frac{\partial \bar{\mathcal{H}}}{\partial x_\mathrm{t}} & \text{if } \mathcal{T}(x_\mathrm{t}) < \mathcal{T}_\mathrm{th} \end{cases} \tag{3.19}$$

The power exchanged between variable spring and tank due to stiffness changes is

$$\dot{\bar{\mathcal{H}}} = \frac{\partial \bar{\mathcal{H}}}{\partial \kappa} \dot{\kappa} = \begin{cases} 0 & \text{if } \mathcal{T}(x_\mathrm{t}) \geq \mathcal{T}_\mathrm{th} \\ \frac{\partial \bar{\mathcal{H}}}{\partial \kappa} \frac{k_{vb}}{\mathcal{T}_{th}} \dot{x}_\mathrm{t} \frac{\partial \bar{\mathcal{H}}}{\partial x_\mathrm{t}} & \text{if } \mathcal{T}(x_\mathrm{t}) < \mathcal{T}_\mathrm{th} \end{cases} \tag{3.20}$$

The power exchanged by the energy tank is of the form $\dot{\mathcal{T}}(x_\mathrm{t}) = \frac{\bar{\mathcal{H}}}{\partial x_\mathrm{t}} f_\mathrm{t}$, therefore $\frac{\partial \bar{\mathcal{H}}}{\partial \kappa} \frac{k_{vb}}{\mathcal{T}_\mathrm{th}} \dot{x}_\mathrm{t}$ is an input for the energy tank. Using these assignments we can write the port-Hamiltonian representation of variable stiffness spring and energy tank. For simplicity we assume that the variable stiffness spring is part of the general system of equation (2.10)

$$\begin{pmatrix} \dot{\boldsymbol{x}} \\ \dot{x}_\mathrm{t} \\ \dot{\kappa} \end{pmatrix} = \left[\begin{pmatrix} J(\boldsymbol{x}) & \frac{\alpha \boldsymbol{w}}{x_\mathrm{t}} & 0 \\ -\frac{\alpha \boldsymbol{w}^T}{x_\mathrm{t}} & 0 & -\frac{k_{vb}}{\mathcal{T}_\mathrm{th}} \dot{x}_\mathrm{t} \\ 0 & \frac{k_{vb}}{\mathcal{T}_\mathrm{th}} \dot{x}_\mathrm{t} & 0 \end{pmatrix} - \begin{pmatrix} R(\boldsymbol{x}) & 0 & 0 \\ -\frac{1}{x_\mathrm{t}} \frac{\partial \bar{\mathcal{H}}^T}{\partial \boldsymbol{x}} R(\boldsymbol{x}) & 0 & 0 \\ 0 & 0 & 0 \end{pmatrix} \right] \begin{pmatrix} \frac{\partial \bar{\mathcal{H}}}{\partial \boldsymbol{x}} \\ \frac{\partial \bar{\mathcal{H}}}{\partial x_\mathrm{t}} \\ \frac{\partial \bar{\mathcal{H}}}{\partial \kappa} \end{pmatrix} \tag{3.21}$$

The combination of such an example system with a variable stiffness spring and a tank is lossless, if we disregard the energy exchange with the robotic environment.

$$\begin{aligned} \frac{d}{dt} \bar{\mathcal{H}}(\boldsymbol{x}, x_\mathrm{t}, \kappa) &= \begin{pmatrix} \frac{\partial^T \bar{\mathcal{H}}}{\partial \boldsymbol{x}} & \frac{\partial^T \bar{\mathcal{H}}}{\partial x_\mathrm{t}} & \frac{\partial^T \bar{\mathcal{H}}}{\partial \kappa} \end{pmatrix} \begin{pmatrix} \dot{\boldsymbol{x}} \\ \dot{x}_\mathrm{t} \\ \dot{\kappa} \end{pmatrix} = \frac{\partial^T \bar{\mathcal{H}}}{\partial \boldsymbol{x}} J(\boldsymbol{x}) \frac{\partial \bar{\mathcal{H}}}{\partial \boldsymbol{x}} + \frac{\partial^T \bar{\mathcal{H}}}{\partial \boldsymbol{x}} \frac{\alpha \boldsymbol{w}}{x_\mathrm{t}} \frac{\partial \bar{\mathcal{H}}}{\partial x_\mathrm{t}} \\ &- \frac{\partial^T \bar{\mathcal{H}}}{\partial \boldsymbol{x}} R(\boldsymbol{x}) \frac{\partial \bar{\mathcal{H}}}{\partial \boldsymbol{x}} - \frac{\partial^T \bar{\mathcal{H}}}{\partial x_\mathrm{t}} \frac{\alpha \boldsymbol{w}^T}{x_\mathrm{t}} \frac{\partial \bar{\mathcal{H}}}{\partial \boldsymbol{x}} - \frac{\partial^T \bar{\mathcal{H}}}{\partial x_\mathrm{t}} \frac{k_{vb}}{T_\mathrm{th}} \dot{x}_\mathrm{t} \frac{\partial \bar{\mathcal{H}}}{\partial \kappa} + \frac{\partial^T \bar{\mathcal{H}}}{\partial x_\mathrm{t}} \frac{1}{x_\mathrm{t}} \frac{\partial^T \bar{\mathcal{H}}}{\partial \boldsymbol{x}} R(\boldsymbol{x}) \frac{\partial \bar{\mathcal{H}}}{\partial \boldsymbol{x}} \\ &+ \frac{\partial^T \bar{\mathcal{H}}}{\partial \kappa} \frac{k_{vb}}{T_\mathrm{th}} \dot{x}_\mathrm{t} \frac{\partial \bar{\mathcal{H}}}{\partial x_\mathrm{t}} = 0 \end{aligned} \tag{3.22}$$

The dissipative structure $R(\boldsymbol{x})$ can be changed without compromising passivity as long as it is positive semi-definite. A change of a damping parameter does not change the energy stored in the system, since dampers do not store energy and do not have a state variable. A similar approach as for stiffness indicates good results in numeric simulations. With a depletion of the energy tank the damping $d_{vb} \in \mathbb{R}^+$ along the user-object spring is reduced, thus the coupling between user and virtual object is further relaxed.

$$\delta = \begin{cases} d_{vb} & \text{if } \mathcal{T}(x_\mathrm{t}) \geq \mathcal{T}_\mathrm{th} \\ d_{vb} \frac{\mathcal{T}(x_\mathrm{t})}{\mathcal{T}_{th}} & \text{if } \mathcal{T}(x_\mathrm{t}) < \mathcal{T}_\mathrm{th} \end{cases} \tag{3.23}$$

3.2.2 Energy exchange with the robotic system and environment

So far we made the simplification of assuming no energy exchange of the controller through the robots with the environment. In contrast to the human-controller relation, the controller-robot relation is established on an energetic level. The robot measures its velocity at exactly the same point it applies the commanded force, this defines the power port between the controller and the robotic environment. The power flow through this port can affect the energy of the tank-controller permanently, i.e. an irreversible drain of energy is possible. In the following three important cases are discussed that interfere with the concept of a constant energy level in tank and controller.
In the controller we assume the robots to be a simple inertia, in reality however they are a system of actuated joints and links with a dynamic behaviour different from a single inertia. To achieve the desired control performance the robots can be precompensated by passive feedback-linearisation [OASK+04]. The internal dynamics and gravity are compensated in favour of shaping a desired inertia. This technique however is passive, but not lossless, because this would require ideal measurements and modelling. This means at this point energy is irreversibly dissipated.
The second issue is the friction in the robot's joints, it can degrade precision and results in a loss of energy seen from the controller-robot power port. In [TASLH08] a passive observer/compensation technique is presented that estimates the torque necessary to overcome friction and applies it in addition. Although this method reduces the energy loss due to friction, it is still a cautious estimation (i.e. passive) and not lossless. Thus, over time the energy stored in robots, controller and energy tank decreases.
A permanent drain of energy in the system occurs, if the robotic system is performing work on the environment. For example, let the common object (connected to the robots) move other objects in the workspace. The work performed on this objects is withdrawn permanently from the energy balance.
Clearly, there is always a drain of energy in a realistic system and at some time the energy tank gets close to depletion. In this case we require a method to restore the capacity to act, by providing energy to the system. It is clear that this means the introduction of a source of energy and thus inflicts a loss of the strict definition of passivity. The safest way of re-powering the system is to allow the operator to supply energy to the tank, in a manner independent of the motion control interface. This means the operator is always in charge of the energy content and is able to estimate the possible impact on the environment. However the approach may be inconvenient, in certain operations the user has to interrupt his actual work and choose an appropriate quantum of energy to send to the energy tank. This may mislead some operators to use higher quanta than those indicated by the safety metrics in section 3.1. Clearly this makes the concept of safety by limited energy ineffective. Therefore an automatic strategy to compensate for energy drain is discussed in the

next subsection.
With no restrictive assumptions on the environment we must consider the case of an environment supplying energy to the robotic system. For safety we suggest to automatically discard energy supplied to the tank that exceeds the initial level.

Automatic compensation for drained energy

The two controllers presented in section 2.6 are based on the model of a cooperative manipulation set-up. In an ideal case the same amount of energy stored in the energy is virtually bound in the controller. I.e. the controller reflects the energy state of the real system. Since all energy sourced by the tank flows through the controller into the robots, bounding the energy in the controller also limits the energy stored in the robotic system. It is thus sufficient to apply the energetic limits, imposed by the safety metrics, to the controller. The proposed automatic compensation re-supplies the energy transferred to the robots into the energy tank. The power exchanged between controller and the i-th robot is defined by the given by the wrench-twist product ${W_i^{0,0}}^T T_i^0$, applying the automatic compensation the energy balance is

$$\dot{\mathcal{T}}(x_\mathrm{t}) + \underbrace{\sum_{i=1}^{n} {W_i^{0,0}}^T T_i^0}_{\text{compensation}} = -\dot{\mathcal{H}}(x) + \sum_{i=1}^{n} {W_i^{0,0}}^T T_i^0 \tag{3.24}$$

This means a constant level of energy in tank and controller $\dot{\mathcal{T}}(x_\mathrm{t}) + \dot{\mathcal{H}} = 0$. Clearly, the compensation term $\sum_{i=1}^{n} {W_i^{0,0}}^T T_i^0$ is active, it provides energy in lieu of the user, who is energetically decoupled in our approach. Still all energy flows through the controller and is bounded if necessary. But the energy budget, given by the tank level, accounts only for the controller state. Please recall that the combination of controller and tank is lossless, so the system can always carry out tasks within the given safety margin.
In order to explain the proposal of enhancing stability and safety by energy-bounding the controller, consider the following illustrative examples. The operator drives the system to a high velocity, due to the moving virtual inertias in the controller, the tank is used up. This leads to a relaxation of the coupling of user and virtual object and prevents prevents further acceleration. Thus the robotic system is kept at a certain speed. This also holds if the virtual inertia parameters deviate from their real pendants (modelling errors). The combination of the initial tank level and the virtual inertias determine the achievable system speed. We can calculate this speed by using the apparent inertia of a cooperative set-up from [EH16].
Please consider again the introductory case of robots driven into an obstacle and a user still to command motion in the blocked direction. The user-object spring is elongated and its potential energy empties the tank. The automatic compensation provides no energy to the tank, because the robots are blocked and do not move, i.e. no power is exchanged. With the depletion of the tank, stiffness and damping of

the user spring are reduced. This keeps the forces bounded even if the user does not change her/his commands. Conclusively the total wrench that the common object can exert on the environment is determined by the initial tank level and the spring stiffness.

Chapter 4

Simulation results

Simulations of the proposed control schemes and existing approaches from literature are conducted to evaluate and compare their effectiveness. The controllers for cooperative manipulation are compared in terms of trajectory tracking, dynamic behaviour and internal stress on the object. To preserve comparability, they are adjusted to exert equal strength of force and the tuning parameters are kept within the same range.
In the simulation the robots we assume the robots to behave like simple inertias, i.e. their underlying dynamics is compensated. The connection between common object (another inertia) and the end-effectors is considered rigid. For the computation of the combined dynamics we apply the principle of constrained motion, explicitly given for a cooperative manipulation set-up in [EH16]. The same article provides the routine used for the calculation of the stress exerted on the object (internal wrench). Simulations are conducted in *MATLAB/Simulink*, using a fixed step solver with a step size of 1ms, this facilitates application in an experimental set-up (the control units typically run at 1kHz). Parameters used in the simulations can be found in table 4.1. The control input is a reference velocity, the set-point position/orientation is computed by integration. Fig. 4.1 shows the two test cases, linear (along the x-axis) and angular velocity (around the z-axis).

Table 4.1: General simulation settings

Number of manipulators	4
Object inertia M_b	1.4 kg $\cdot I_3$ (lin.), 0.2 kgm^2 $\cdot\, I_3$ (ang.)
Manipulator inertia M_i	10 kg $\cdot I_3$ (lin.), 0.5 kgm^2 $\cdot\, I_3$ (ang.)
Object diameter	0.8m

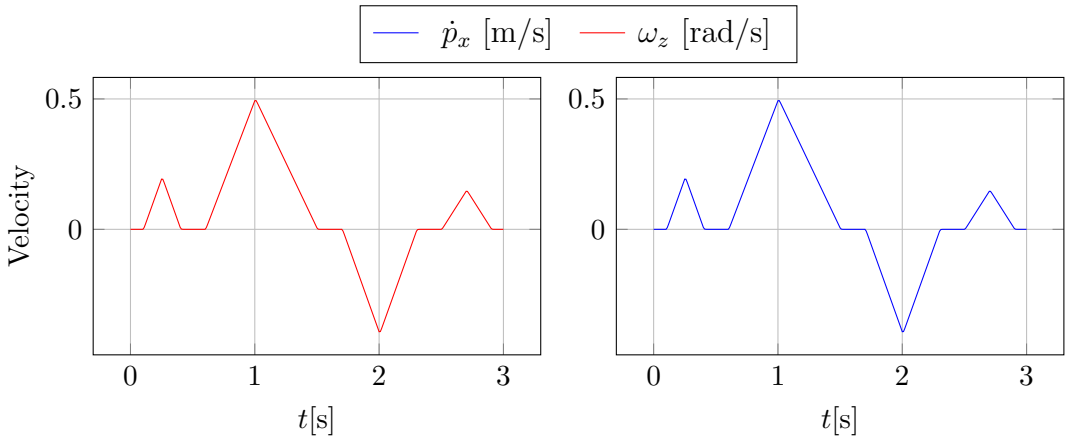

Figure 4.1: Test reference trajectories for translation (left) and rotation

4.1 State-of-the-art control schemes for cooperative manipulation

4.1.1 Internal and external impedance based reference trajectory generation

A renowned approach by Caccavale and Villani [CV01, CCMV08] consists of a cascaded architecture enforcing two impedance relations. One is established between the given reference trajectory and the object, we refer to an *external* impedance. The other is between the manipulators and the object and is called *internal*. The output of the impedance loops is a compliant reference trajectory which is used in an *inner motion control* loop to generate forces to drive the robot. The parameters used in the simulation are chosen very close to the ones given in [CCMV08], see table 4.2.
The simulation results are presented in figure 4.1.1, the left column shows the linear motion test case and the right the rotational one. The plots on top show the deviation from the desired position and orientation respectively. Below the velocity

Table 4.2: Parameters for dual impedance controlled reference trajectory generation

	linear	angular
Ext. inertia	$0.7\text{kg} \cdot I_3$	$0.1\text{kgm}^2 \cdot I_3$
Ext. damping	$1500\text{kg/s} \cdot I_3$	$10\text{kgm}^2/\text{s} \cdot I_3$
Ext. stiffness	$700\text{N/m} \cdot I_3$	$5\text{Nm} \cdot I_3$
Int. inertia	$10\text{kg} \cdot I_3$	$0.5\text{kgm}^2 \cdot I_3$
Int. damping	$1000\text{kg/s} \cdot I_3$	$80\text{kgm}^2/\text{s} \cdot I_3$
Int. stiffness	$400\text{N/m} \cdot I_3$	$2\text{Nm} \cdot I_3$

Table 4.3: Parameters for the internal impedance control with object dynamics feed-forward

	linear	angular
Object inertia ff.	$1.4\text{kg} \cdot I_3$	$0.2\text{kgm}^2 \cdot I_3$
Int. inertia	$10\text{kg} \cdot I_3$	$0.5\text{kgm}^2 \cdot I_3$
Int. damping	$1000\text{kg/s} \cdot I_3$	$80\text{kgm}^2/\text{s} \cdot I_3$
Int. stiffness	$400\text{N/m} \cdot I_3$	$2\text{Nm} \cdot I_3$

errors are displayed. The third plot row shows the wrenches applied by one of the manipulators. The bottom row indicates the internal stress a manipulator exerts on the object.
The approach shows good trajectory tracking, especially the velocity error is the lowest in this comparative study. The internal wrench is low and is similar to the other approaches, for linear motion not any internal stress occurs.

4.1.2 Internal impedance control with feed-forward of the object dynamics

Erhart and Hirche [EH16] omit the external impedance relation and but include object dynamics feed-forward. I.e. the wrench necessary to accelerate the object's inertia is distributed by an inverse of the grasp matrix to the manipulators. This results in even better position/orientation accuracy compared to the previous. However results presented in [CCMV08] indicate that, in absence of an external impedance relation, higher forces occur, if the object comes into contact with the environment. Interestingly the magnitude of the internal forces (during rotation) depends directly on the step size of the simulation (running a fixed step solver), i.e. a ten-times smaller step size gives ten-times smaller internal forces. Internal forces are calculated based on the geometry in the last simulation step. The correlation between step size and values indicates that these forces are rather due to the discrete nature of the simulation than of the control law generating internal stress.
Table 4.3 shows the parameters used and the results can be seen from figure 4.1.2.

4.1.3 Classic IPC by Stramigioli

The IPC was introduced by Stramigioli [Str01b] and experimentally evaluated by Wimböck et al. [WOH08] on a robotic hand. In Stramigioli's version there are no dampers along the manipulator-object springs and Wimboeck uses only translational springs. The simulation results presented here are a combination of both implementations, we use dampers along 6-DoF springs. the architecture has been detailed throughout this work.
The impedance parameters are chosen equal or lower for translation and significantly

Table 4.4: Parameters for the IPC

	linear	angular
Virt. inertia	$1.4\text{kg} \cdot I_3$	$0.2\text{kgm}^2 \cdot I_3$
Ext. damping	$1500\text{kg/s} \cdot I_3$	$500\text{kgm}^2/\text{s} \cdot I_3$
Ext. stiffness	$700\text{N/m} \cdot I_3$	$400\text{Nm} \cdot I_3$
Int. damping	$625\text{kg/s} \cdot I_3$	$31.25\text{kgm}^2/\text{s} \cdot I_3$
Int. stiffness	$125\text{N/m} \cdot I_3$	$6.25\text{Nm} \cdot I_3$

higher for rotation, see table 4.4. The results (fig. 4.1.3) show a clearly inferior trajectory tracking compared to the previous approaches. This stems from a different mode of function of the inertias in the IPC. In classic impedance control clearly the inertia is in parallel with the spring and in the IPC the inertia is connected in series, figure 4.4 illustrates the concepts. In the first case the inertia is used to calculate the wrench necessary to accelerate the associated body, in the latter the spring and damper need to provide the wrench to accelerate the additional (virtual) body. Thus the inertia in the IPC is an energy storing element that reduces the controller dynamics. On the other hand the IPC does not require absolutely smooth reference velocities. The classic impedance control approaches use the time-derivative of the input velocity and often require pretreatment (e.g. low-pass filtering) of the input.

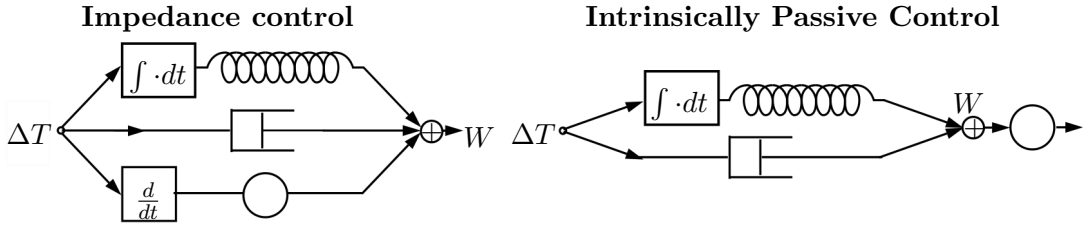

Figure 4.4: Arrangement of spring, mass and damper in classical impedance control approaches and in the IPC

The feasible stiffness and damping in this implementation is limited by numerical stability, a further increase leads to infinite values at some point of the simulation. This issue also requires the use of *Simulink's ode8* solver for this approach, instead of *ode1* (Euler's method) used for the other simulations. The *ode8* method is of the *Dormand-Prince* class with an accuracy order of 8. The rate of rate of convergence improves at the cost of higher computational complexity [Mat16].

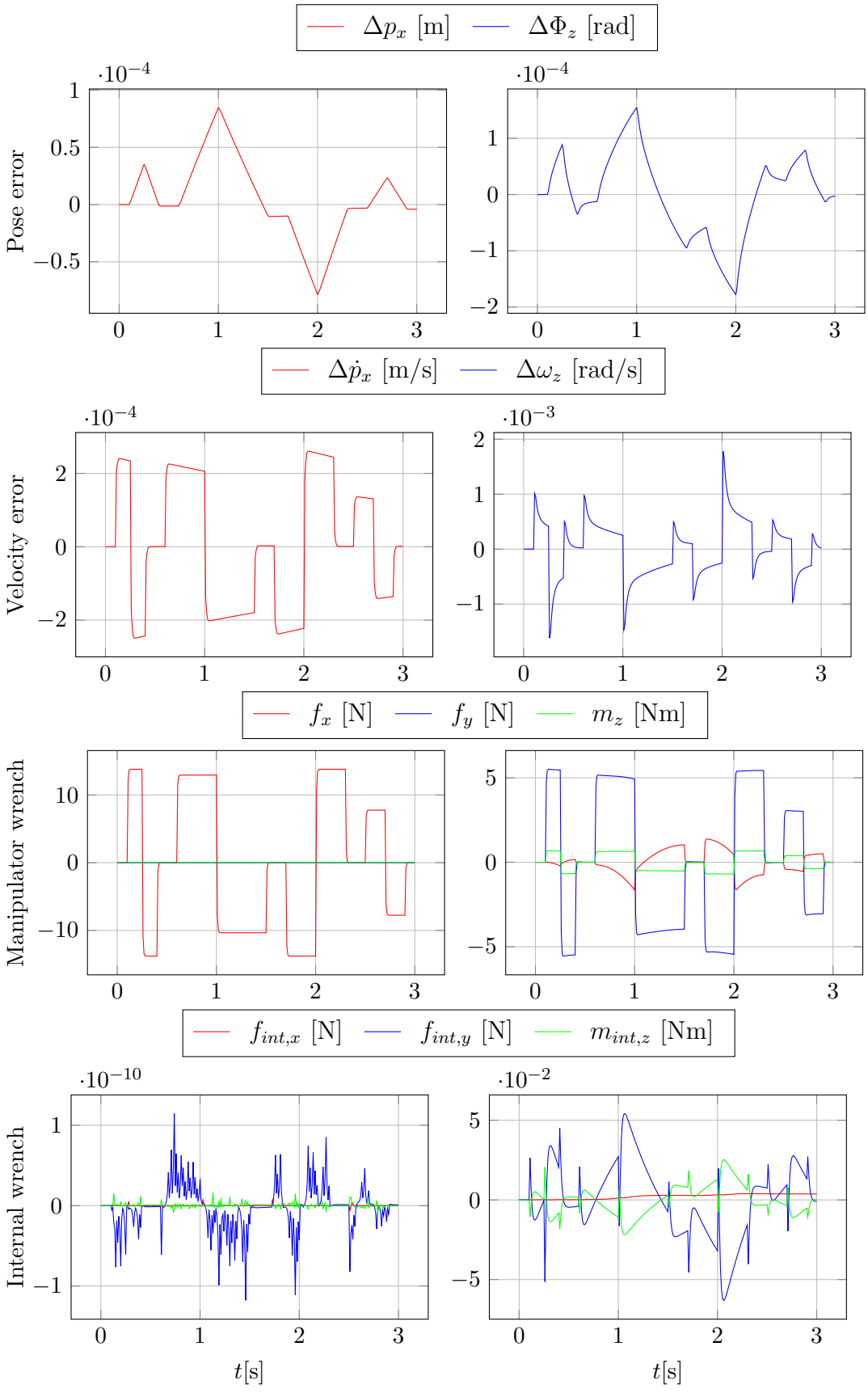

Figure 4.2: Internal and external impedance based reference trajectory generation: Translation (left column) and rotation

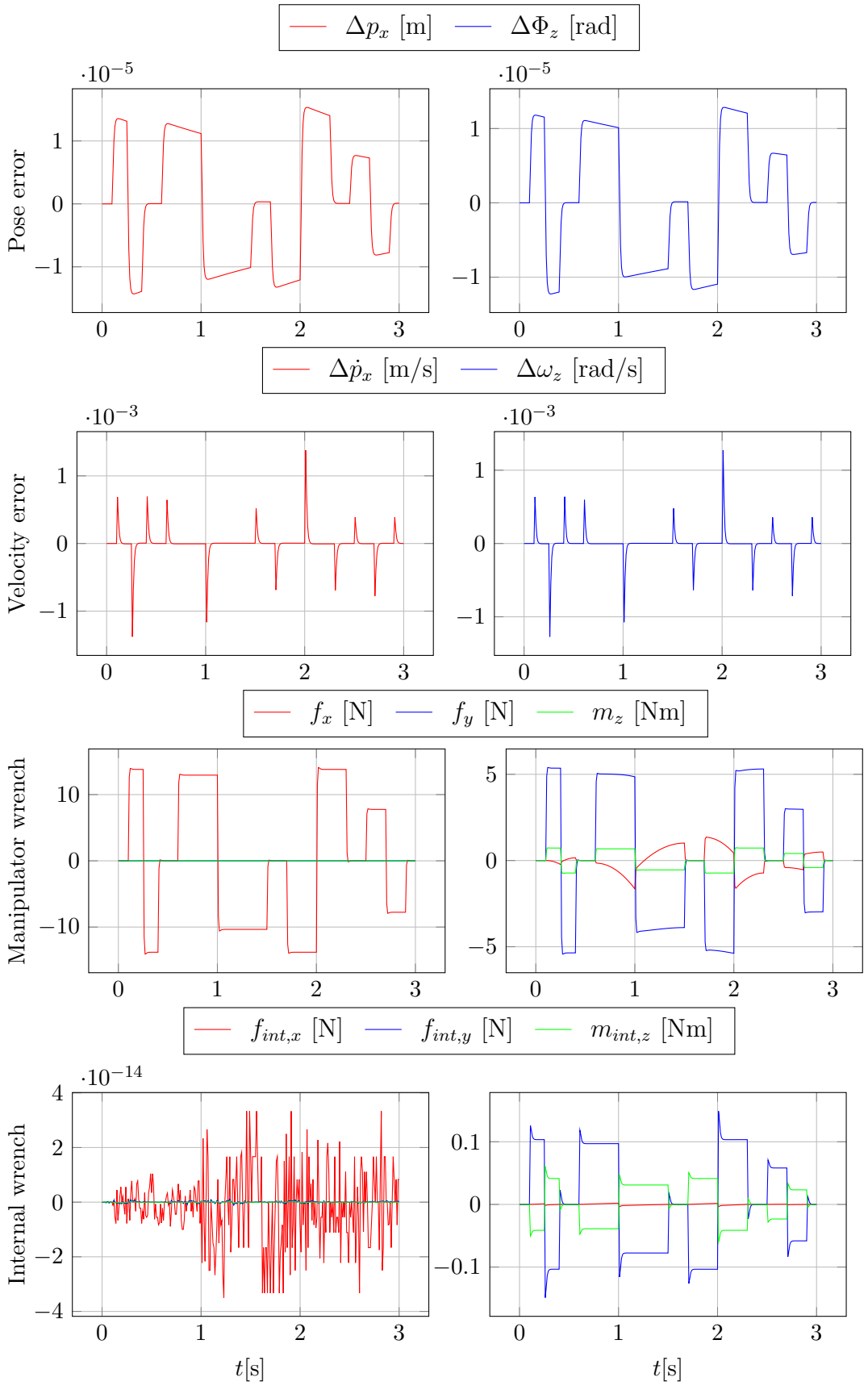

Figure 4.3: Internal impedance control with feed-forward of the object dynamics: Translation (left column) and rotation

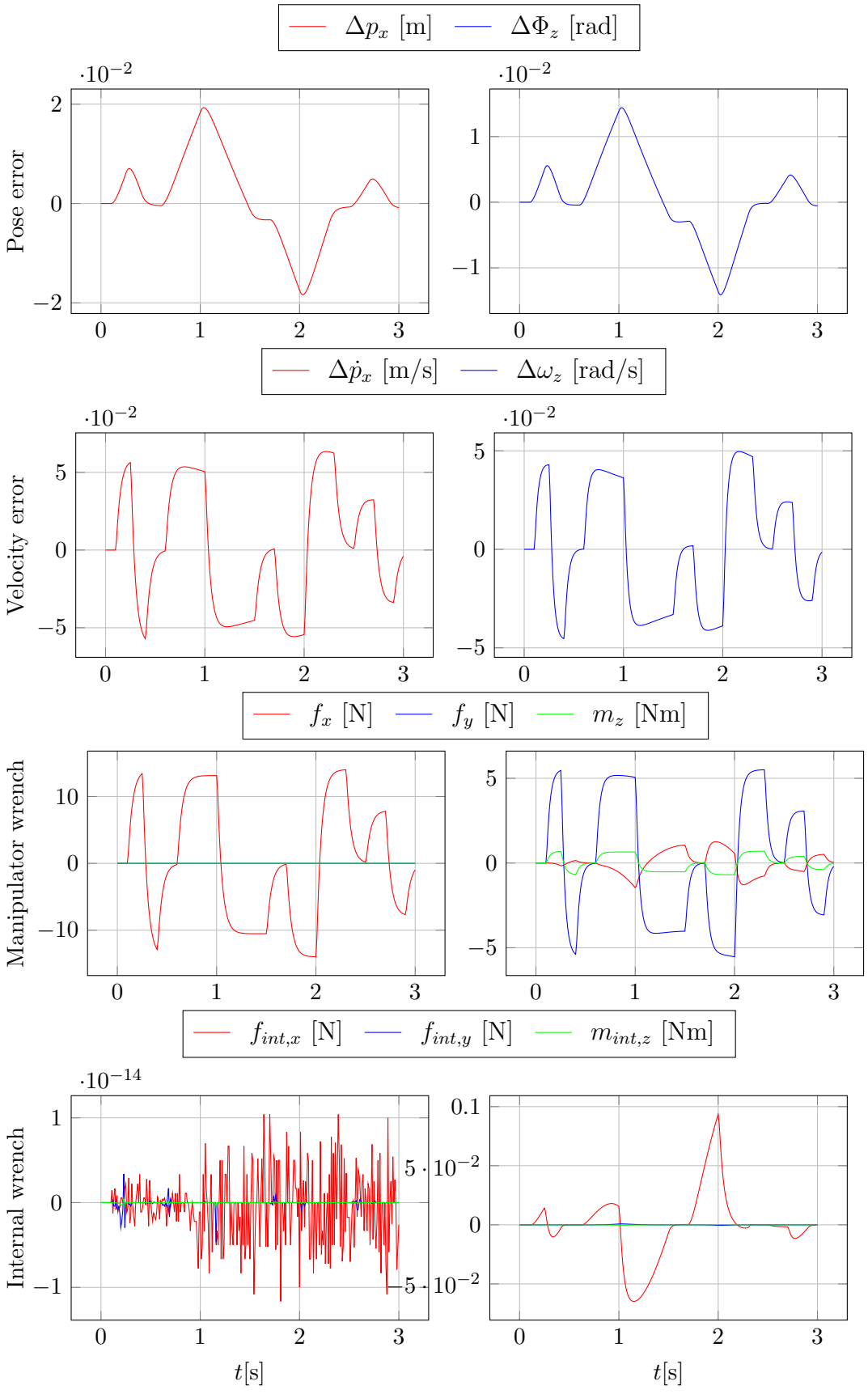

Figure 4.5: Intrinsically Passive Controller: Translation (left column) and rotation

Table 4.5: Parameters for the constrained dynamic IPC

	linear	angular
Virt. object inertia	$1.4\text{kg} \cdot I_3$	$0.2\text{kgm}^2 \cdot I_3$
Virt. manipulator inertia	$0.5\text{kg} \cdot I_3$	$0.25\text{kgm}^2 \cdot I_3$
Ext. damping	$1500\text{kg/s} \cdot I_3$	$1500\text{kgm}^2/\text{s} \cdot I_3$
Ext. stiffness	$700\text{N/m} \cdot I_3$	$700\text{Nm} \cdot I_3$
Int. damping	$900\text{kg/s} \cdot I_3$	$45\text{kgm}^2/\text{s} \cdot I_3$
Int. stiffness	$180\text{N/m} \cdot I_3$	$9\text{Nm} \cdot I_3$

4.2 Simulation of the constrained dynamics IPC

The implementation of the constrained dynamics IPC as proposed in section 2.6 does not suffer from numerical issues as the classic IPC. This allows to increase the angular stiffness and damping and achieve a better dynamic performance for an angular motion. The simulation results are shown in figure 4.2. Note that including the inertias of the manipulators in the controller introduces further energy storing elements, i.e. makes the controller more inert. The better trajectory tracking (especially in angular motion) in comparison to the classic IPC results from the higher parameters, which are reported in table 4.5. By choosing the controller manipulator inertia lower than in the robotic system the dynamic response can be improved. The angular velocity deviation is halved in comparison to the classic IPC, but still approximately 20 times higher than in the impedance control approaches. All controllers are tuned to command the same magnitude of force to the robots, the deviations in tracking behaviour result from different force gradients.

4.3 Compliant trajectory generating IPC

The compliant trajectory generating IPC uses an force control loop to compute the force commands for the robots. The structure can either be viewed as PI-control or as a spring and a damper in parallel. Gains or stiffness/damping can be chosen high because the superimposed control scheme already establishes compliance [CCMV08], the simulation settings are summarized in table 4.6. Numerical stability problems also occur with this approach, the reported parameters the maximum feasible with a fixed step solver (*ode8*) at 1 ms step size. With a variable step solver (e.g. *ode45*) higher stiffness and damping are reachable and performance is superior. Due to non-applicability in real robotic system, these solvers are not considered further. Stiffness and damping is similar to the classic IPC parameters, the dynamic performance is inferior because of the additional inertias, which have to be accelerated. This results in approx. double errors in position/orientation and velocity compared to the classic IPC, see figure 4.3, In contrast to the constrained dynamic IPC the virtual inertias for the object and the manipulators cannot be chosen smaller than their real

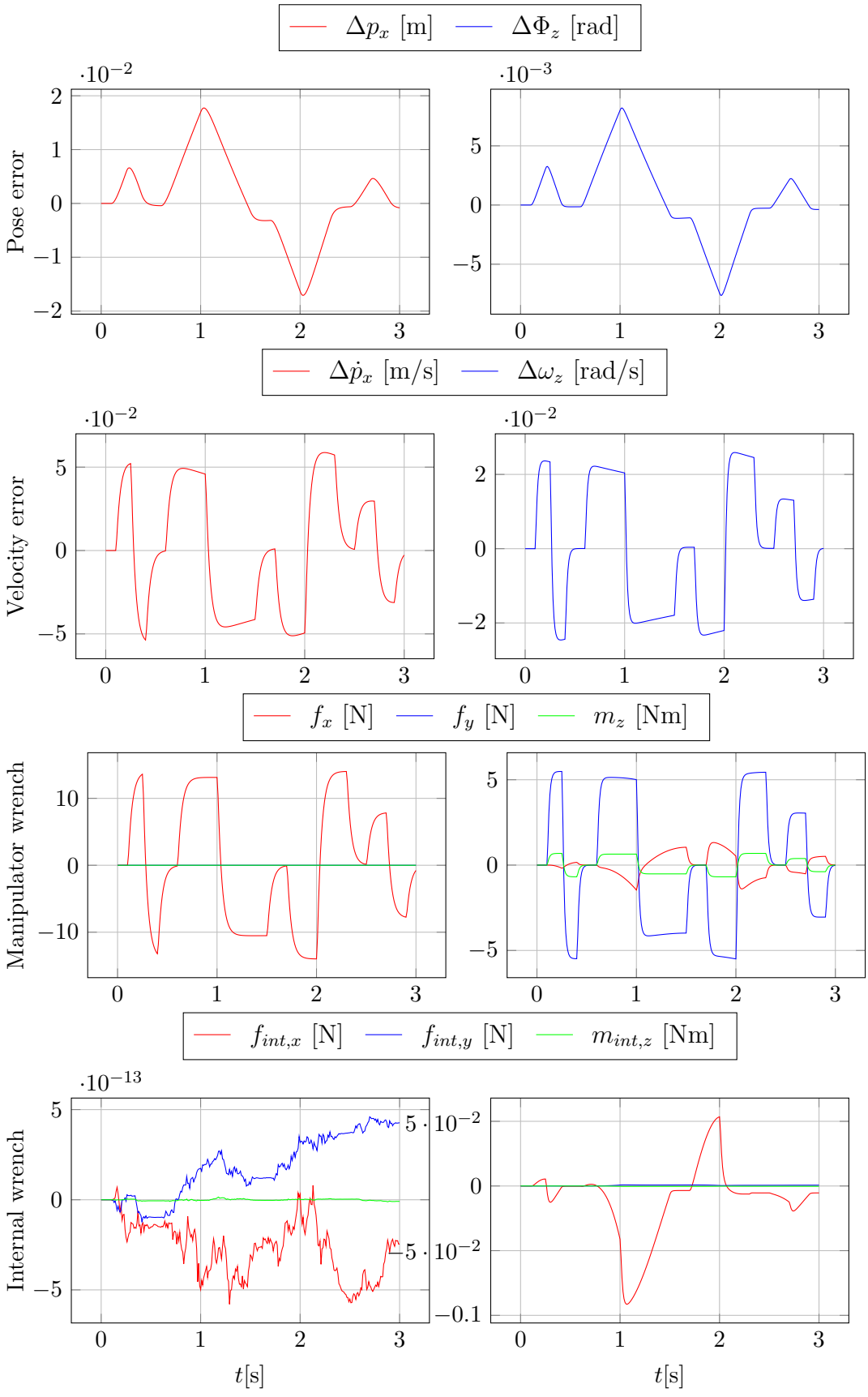

Figure 4.6: Constrained dynamic IPC: Translation (left column) and rotation

Table 4.6: Parameters for the compliant trajectory generating IPC

	linear	angular
Virt. object inertia	$1.4\text{kg} \cdot I_3$	$0.2\text{kgm}^2 \cdot I_3$
Virt. manipulator inertia	$10\text{kg} \cdot I_3$	$0.5\text{kgm}^2 \cdot I_3$
Ext. damping	$1500\text{kg/s} \cdot I_3$	$500\text{kgm}^2/\text{s} \cdot I_3$
Ext. stiffness	$700\text{N/m} \cdot I_3$	$400\text{Nm} \cdot I_3$
Int. damping	$600\text{kg/s} \cdot I_3$	$30\text{kgm}^2/\text{s} \cdot I_3$
Int. stiffness	$120\text{N/m} \cdot I_3$	$6\text{Nm} \cdot I_3$
Force control damping	$5000\text{kg/s} \cdot I_3$	$1500\text{kgm}^2/\text{s} \cdot I_3$
Force control stiffness	$500\text{N/m} \cdot I_3$	$200\text{Nm} \cdot I_3$

pendants. Doing so leads to infinite simulation results. This entails in an even wider performance gap to the constrained dynamic IPC.

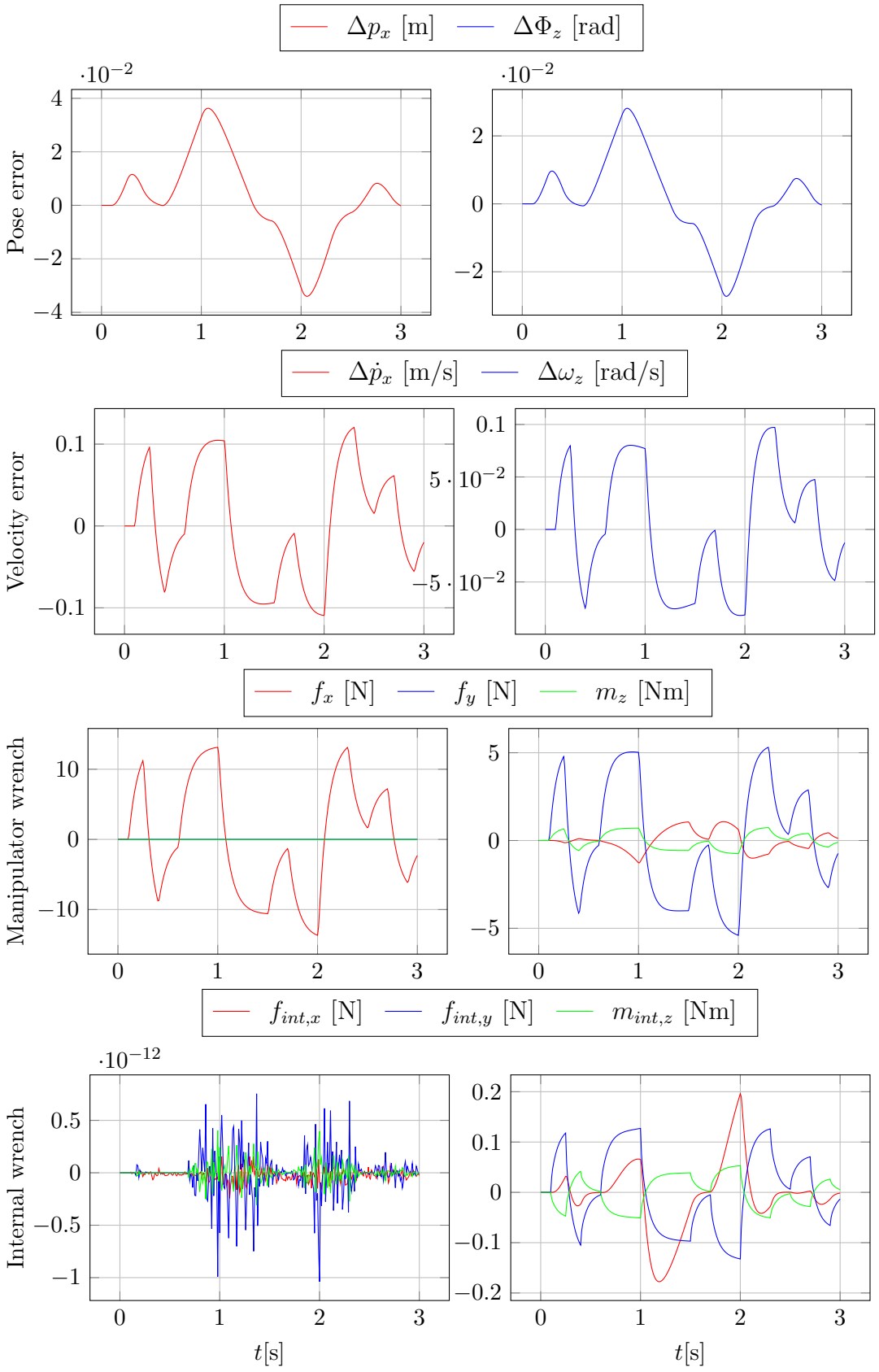

Figure 4.7: Compliant reference trajectory generating IPC: Translation (left column) and rotation

4.4 Energy-bounded trajectory tracking

In the presented simulation, trajectory tracking demands more energy than is available from the energy tank (detailed in section 3.2). The budget for performing operations is limited to 30 J, in accordance with the safety limit of neck fractures (see section 3.1). Trajectories exceeding this limit are adapted with a the variable stiffness and damping technique presented in subsection 3.2.1. The underlying control scheme is the dynamic constrained IPC from section 2.6.
In the simulation we assume that no energy is lost in the robotic system (due to friction or work on the environment). If the user commands acceleration, energy is transferred from the tank through the controller into the robotic system and is thereby stored in form of potential and energy. When the system slows down, the kinetic and potential energy is is re-transformed into free energy and stored in the tank. This happens in an ideal, lossless way, thus the energy tank reaches the former level after an operation, see the third plot in figure 4.4. Upon depletion of the tank (approx. at $t = 2$ s), the kinetic energy cannot be further increased and the velocity stays constant (observable from the second plot). The reduction of stiffness and damping starts as soon as the level falls under a certain threshold, here $T_{th} = 10$ J. As a consequence from $t = 1.7$ s on the velocity increases slower. The actual position falls behind the desired (first plot in figure 4.4), with the reduced velocity it takes until $t = 2.6$ s to catch up to the desired position. During this time the velocity is kept at the energetically feasible maximum. As soon as the velocity reduces the energy level recovers quickly. The approach attempts optimal position tracking under the given energy constraint and no permanent deviations occur after the energetic level has recovered.

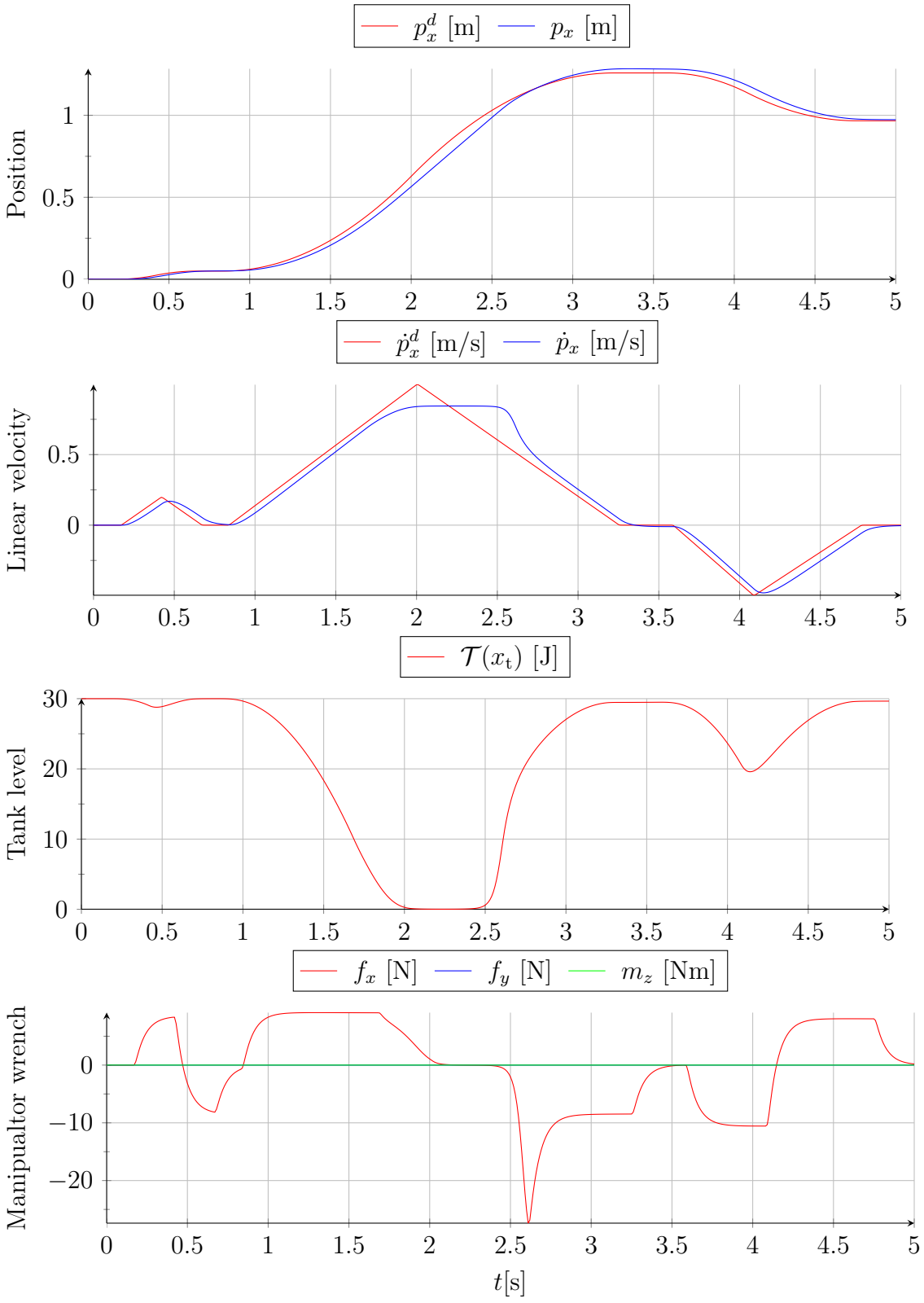

Figure 4.8: Energy bounding by a variable stiffness spring and a variable damper

Chapter 5

Conclusion

Cooperative manipulation is analysed for the first time in the port-Hamiltonian setting. We provide a self-contained derivation of the constraint forces arising when the manipulators are rigidly connected to the common object. We show that these forces do not generate, store or dissipate energy, i.e. the rigid connection is energy consistent. The modelling of the rigid connections is also used for control.
Two model-based controllers are designed for the teleoperated, shared control task of cooperative object manipulation. Their main characteristic is the virtual structure that resembles an impedance-controlled cooperative manipulation set-up. The design is based on physical intuition and is intrinsically passive.
Simulation results show that the dynamic response of the proposed controllers is inferior by one order of magnitude, compared to classic cooperative manipulation approaches. Stramigioli's IPC has a similar architecture and the performance compares well to our controllers. Classic cooperative manipulation approaches use the desired acceleration to calculate the forces necessary to speed up the inertias in the set-up. The proposed controllers and the IPC do not, plus have additional virtual inertias that retard dynamic motion. In the simulations the classic IPC and the reference trajectory generating controller suffer from numeric instabilities, the constrained dynamics IPC does not and is therefore preferred for safety concerns.
Input interfaces, that do not impose a counteracting force or have deflection barriers, allow a human to issue arbitrary commands, which may be unstable and/or unsafe. The model-based control design on energetic level calculates the energetic state of the controller, which directly reflects the situation in the real set-up. This allows to distinguish between energy appropriately spent on the task and energy driving the system to a potentially harmful state. The latter type is kept bounded by energy shaping control, i.e. dynamically adapting the controller parameters.
The controlled robotic system is sourced from an energy tank, the energy supplied to the robots is re-fed into the tank, i.e. the controller energy level is bounded. Through the automatic re-filling an infinite amount of energy may be supplied over time. Then the robots do not reach an energetic minimum. Thus we cannot conclude asymptotic stability, which follows from a passive robotic system with a finite

supply of energy. However by bounding the energy in the controller the energy in the real set-up gets also limited and the system is at a stable energetic state. This is valid if the environment provides only a finite amount of energy.
Limiting the energy, also restricts the possible impact in case of a collision with a human or the environment. The prime task in cooperative manipulation is the transportation of large and/or heavy objects, usually this is carried out at low speeds. Injuries due to violent pressure on a clamped human may be more relevant in this set-up. The proposed energy shaping approach also limits the possible force, but the used safety metrics should be analysed especially for this case.

List of Figures

Bibliography

[BH96] R.G. Bonitz and T.C. Hsia. Internal force-based impedance control for cooperating manipulators. *IEEE Transactions on Robotics and Automation*, 12(1):78–89, Feb 1996. doi:10.1109/70.481752.

[CCMV08] F. Caccavale, P. Chiacchio, A. Marino, and L. Villani. Six-dof impedance control of dual-arm cooperative manipulators. *IEEE/ASME Transactions on Mechatronics*, 13(5):576–586, 2008. doi:10.1109/TMECH.2008.2002816.

[CM08] F. Caccavle and Uchiyama M. Cooperative manipulation. In Bruno Siciliano and Oussama Khatib, editors, *Springer Handbook of Robotics*, chapter 29, pages 701–718. Springer, 2008. doi:10.1007/978-3-540-30301-5.

[CV01] F. Caccvale and L. Villani. An impedance control strategy for cooperative manipulation. In *Proc. IEEE/ASME Int. Conf. on Advanced Intelligent Mechatronics*, volume 1, pages 343–348, 2001. doi:10.1109/AIM.2001.936478.

[DMSB09] V. Duindam, A. Macchelli, S. Stramigioli, and H. Bruyninckx. *Modeling and Control of Complex Physical Systems*. Springer, 2009. doi:10.1007/978-3-642-03196-0.

[DS09] V. Duindam and S. Stramigioli. *Modeling and Control for Efficient Bipedal Walking Robots*, volume 53 of *Springer Tracts in Advanced Robotics*. Springer, 2009. doi:10.1007/978-3-540-89918-1.

[EH16] S. Erhart and S. Hirche. Model and analysis of the interaction dynamics in cooperative manipulation tasks. *IEEE Transactions on Robotics*, 2016.

[FSM+11] M. Franken, S. Stramigioli, S. Misra, C. Secchi, and A. Macchelli. Bilateral telemanipulation with time delays: A two-layer approach combining passivity and transparency. *IEEE Transactions on Robotics*, 27(4):741–756, Aug 2011. doi:10.1109/TRO.2011.2142430.

[GFS+14] G. Gioioso, A. Franchi, G. Salvietti, S. Scheggi, and D. Prattichizzo. The flying hand: A formation of UAVs for cooperative aerial telemanipulation. In *Proc. IEEE Int. Conf. on Robotics and Automation*, pages 4335–4341, May 2014. doi:10.1109/ICRA.2014.6907490.

[Goe52] R.C. Goertz. Fundamentals of general-purpose remote manipulators. *Nucleonics*, 10(11):36–45, 1952.

[GSDLP16] M. Geravand, E. Shahriari, A. De Luca, and A. Peer. Port-based Modeling of Human-Robot Collaboration towards Safety-enhancing Energy Shaping Control. In *Proc. IEEE Int. Conf. on Robotics and Automation*, 2016. accepted for publication.

[Had14] Sami Haddadin. *Towards Safe Robots - Approaching Asimov's 1st Law*, volume 90 of *Springer Tracts in Advanced Robotics*. Springer, 2014. doi:10.1007/978-3-642-40308-8.

[HB12] S. Hirche and M. Buss. Human-oriented control for haptic teleoperation. *Proceedings of the IEEE*, 100(3):623–647, March 2012. doi:10.1109/JPROC.2011.2175150.

[HKDN13] D. Heck, D. Kostic, A. Denasi, and H. Nijmeijer. Internal and external force-based impedance control for cooperative manipulation. In *Proc. European Control Conference*, pages 2299–2304, July 2013.

[Hog84a] Neville Hogan. Adaptive control of mechanical impedance by coactivation of antagonist muscles. *IEEE Transactions on Automatic Control*, 29(8):681–690, Aug 1984. doi:10.1109/TAC.1984.1103644.

[Hog84b] Neville Hogan. Impedance control: An approach to manipulation. In *American Control Conference*, pages 304–313, June 1984.

[Hog89] Neville Hogan. Controlling impedance at the man/machine interface. In *Proc. IEEE Int. Conf. on Robotics and Automation*, pages 1626–1631 vol.3, May 1989. doi:10.1109/ROBOT.1989.100210.

[Ind14] Mitsubishi Heavy Industries. "MEISTeR" Remote Control Robot Completes Demonstration Testing At Fukushima Daiichi Nuclear Power Station, 2014. Press Information 1775, February 20, 2014; Online, accessed January 13, 2016. URL: https://www.mhi-global.com/news/story/1402201775.html.

[LBY03] J. R. T. Lawton, R. W. Beard, and B. J. Young. A decentralized approach to formation maneuvers. *IEEE Transactions on Robotics and Automation*, 19(6):933–941, Dec 2003. doi:10.1109/TRA.2003.819598.

[LH10] D. Lee and K. Huang. Passive-set-position-modulation framework for interactive robotic systems. *IEEE Transactions on Robotics*, 26(2):354–369, April 2010. doi:10.1109/TRO.2010.2041877.

[LL02] G. Liu and Z. Li. A unified geometric approach to modeling and control of constrained mechanical systems. *IEEE Transactions on Robotics and Automation*, 18(4):574–587, Aug 2002. doi:10.1109/TRA.2002.802207.

[LS05] D. Lee and M.W. Spong. Bilateral teleoperation of multiple cooperative robots over delayed communication networks: Theory. In *Proc. IEEE Int. Conf. Robotics and Automation*, pages 360–365, April 2005. doi:10.1109/ROBOT.2005.1570145.

[LTC09] M. Laffranchi, N. G. Tsagarakis, and D. G. Caldwell. Safe human robot interaction via energy regulation control. In *Proc. IEEE/RSJ Int. Conf. on Intelligent Robots and Systems*, pages 35–41, Oct 2009. doi:10.1109/IROS.2009.5354803.

[LTC12] M. Laffranchi, N. G. Tsagarakis, and D. G. Caldwell. Improving safety of human-robot interaction through energy regulation control and passive compliant design. In Maurtua Inaki, editor, *Human Machine Interaction - Getting Closer*, chapter 8, pages 155–170. InTech, 2012. doi:10.5772/1349.

[Mat16] MathWorks. Choose a Solver, 2016. Simulink Documentation R2016a, online, accessed April 23, 2016. URL: http://de.mathworks.com/help/simulink/ug/types-of-solvers.html.

[NPH08] G. Niemeyer, C. Preusche, and G. Hirzinger. Telerobotics. In Bruno Siciliano and Oussama Khatib, editors, *Springer Handbook of Robotics*, chapter 31, pages 741–757. Springer, 2008. doi:10.1007/978-3-540-30301-5.

[OASK+04] C. Ott, A. Albu-Schaffer, A. Kugi, S. Stamigioli, and G. Hirzinger. A passivity based cartesian impedance controller for flexible joint robots - part i: torque feedback and gravity compensation. In *Proc. IEEE Int. Conf. on Robotics and Automation*, volume 3, pages 2659–2665, April 2004. doi:10.1109/ROBOT.2004.1307462.

[OvdSME99] R. Ortega, A. J. van der Schaft, B. Maschke, and G. Escobar. Energy-shaping of port-controlled hamiltonian systems by interconnection. In *Proc. IEEE Conf. on Decision and Control*, volume 2, pages 1646–1651 vol.2, 1999. doi:10.1109/CDC.1999.830260.

[OvdSMM01] R. Ortega, A. J. van der Schaft, I. Mareels, and B. Maschke. Putting energy back in control. *IEEE Control Systems Magazine*, 21(2):18–33, Apr 2001. doi:10.1109/37.915398.

[PST+15] J. R. Peters, V. Srivastava, G. S. Taylor, A. Surana, M. P. Eckstein, and F. Bullo. Human supervisory control of robotic teams: Integrating cognitive modeling with engineering design. *IEEE Control Systems Magazine*, 35(6):57–80, Dec 2015. doi:10.1109/MCS.2015.2471056.

[SC92] S.A. Schneider and R.H. Cannon. Object impedance control for cooperative manipulation: theory and experimental results. *IEEE Transactions on Robotics and Automation*, 8(3):383–394, 1992. doi:10.1109/70.143355.

[SD01] S. Stramigioli and V. Duindam. Variable spatial springs for robot control applications. In *Proc. IEEE/RSJ Int. Conf. on Intelligent Robots and Systems*, volume 4, pages 1906–1911, 2001. doi:10.1109/IROS.2001.976352.

[She92] T.B. Sheridian. *Telerobotcis, Automation and Human Supervisory Control*. MIT Press, Cambridge, 1992.

[SMA99] S. Stramigioli, Claudio Melchiorri, and S. Andreotti. A passivity-based control scheme for robotic grasping and manipulation. In *Proc. IEEE Conf. on Decision and Control*, volume 3, pages 2951–2956, 1999. doi:10.1109/CDC.1999.831385.

[SMH15] D. Sieber, S. Music, and S. Hirche. Multi-robot manipulation controlled by a human with haptic feedback. In *Proc. IEEE/RSJ Int. Conf. on Intelligent Robots and Systems*, pages 2440–2446, Sep 2015. doi:10.1109/IROS.2015.7353708.

[SMP14] S. Scheggi, F. Morbidi, and D. Prattichizzo. Human-robot formation control via visual and vibrotactile haptic feedback. *IEEE Transactions on Haptics*, 7(4):499–511, Oct 2014. doi:10.1109/TOH.2014.2332173.

[Str01a] Stefano Stramigioli. Geometric modeling of mechanical systems for interactive control. In Alfonso Banos, Francoise Lamnabhi-Lagarrigue, and Francisco J. Montoya, editors, *Advances in the control of nonlinear systems*, volume 264 of *Lecture Notes in Control and Information Sciences*, pages 309–332. Springer, 2001. doi:10.1007/BFb0110375.

[Str01b] Stefano Stramigioli. *Modeling and IPC Control of Interactive Mechanical Systems: A Coordinate-Free Approach*, volume 266 of *Lecture Notes in Control and Information Sciences*. Springer, 2001. doi:10.1007/BFb0110400.

[Str15] Stefano Stramigioli. Energy-aware robotics. In M. K. Camlibel, A. A. Julius, R. Pasumarthy, and J. Scherpen, editors, *Mathematical Control Theory I*, volume 461 of *Lecture Notes in Control and Information Sciences*, pages 37–50. Springer, 2015. doi:10.1007/978-3-319-20988-3.

[TASLH08] L. Le Tien, A. Albu-Schaffer, A. De Luca, and G. Hirzinger. Friction observer and compensation for control of robots with joint torque measurement. In *Proc. IEEE/RSJ Int. Conf. on Intelligent Robots and Systems*, pages 3789–3795, Sept 2008. doi:10.1109/IROS.2008.4651049.

[TdVS14] T. S. Tadele, T. J. A. de Vries, and S. Stramigioli. Combining energy and power based safety metrics in controller design for domestic robots. In *2014 IEEE International Conference on Robotics and Automation (ICRA)*, pages 1209–1214, May 2014. doi:10.1109/ICRA.2014.6907007.

[vdS06] Arjan J. van der Schaft. Port-hamiltonian systems: an introductory survey. In M. Sanz-Sole, J. Soria, J.L. Varona, and J. Verdera, editors, *Proc. Int. Congress of Mathematicians Vol. III: Invited Lectures*, pages 1339–1365, Madrid, Spain, 2006. European Mathematical Society Publishing House.

[vdS13] Arjan J. van der Schaft. Port-hamiltonian differential-algebraic systems. In A. Ilchmann and T. Reis, editors, *Surveys in Differential-Algebraic Equations I*, pages 173–226. Springer, 2013. doi:10.1007/978-3-642-34928-7.

[vdSJ14] A. J. van der Schaft and Dimitri Jeltsema. *Port-Hamiltonian Systems Theory: An Introductory Overview*. Foundations and Trends in Systems and Control. NOW Publishing Inc., Hanover, MA, 2014. doi:10.1561/2600000002.

[VSvdSP14] Ewoud Vos, Jacquelien M.A. Scherpen, A. J. van der Schaft, and Ate Postma. Formation control of wheeled robots in the port-hamiltonian framework. In *World Congress of the International Federation of Automatic Control (IFAC)*, volume 19, pages 6662–6667, 2014. doi:10.3182/20140824-6-ZA-1003.00394.

[WOH06] T. Wimboeck, C. Ott, and G. Hirzinger. Passivity-based object-level impedance control for a multifingered hand. In *Proc. IEEE/RSJ Int. Conf. on Intelligent Robots and Systems*, pages 4621–4627, Oct 2006. doi:10.1109/IROS.2006.282170.

[WOH08] T. Wimboeck, C. Ott, and G. Hirzinger. Analysis and experimental evaluation of the intrinsically passive controller (ipc) for multifingered hands. *Porc. IEEE Int. Conf. on Robotics and Automation*, pages 278–284, May 2008. doi:10.1109/ROBOT.2008.4543221.

[Woo71] Jack L. Wood. Dynamic response of human cranial bone. *Journal of Biomechanics*, 4(1):1 – 12, 1971. doi:10.1016/0021-9290(71)90010-8.

[WS08] K. Waldron and J. Schmiedeler. Kinematics. In Bruno Siciliano and Oussama Khatib, editors, *Springer Handbook of Robotics*, chapter 1, pages 9–33. Springer, 2008. doi:10.1007/978-3-540-30301-5.

[YPM+96] N. Yoganandan, F.A. Pintar, D.J. Maiman, J.F. Cusick, A. Sances, and P.R. Walsh. Human head-neck biomechanics under axial tension. *Medical Engineering and Physics*, 18(4):289 – 294, June 1996. doi:10.1016/1350-4533(95)00054-2.

License